AGU PUBLICATIONS

JGR

Journal of Geophysical Research: Atmospheres

RESEARCH ARTICLE

10.1002/2013JD021433

Key Points:
- Submillimeter ClO measurements across the terminator in three Arctic winters are analyzed
- Only ClO-dimer cross sections leading to fast photolysis are plausible
- Calculations with the JPL recommendation of Keq agree well with observed ClO

Supporting Information:
- Readme
- Figure S1
- Figure S2

Correspondence to:
A. Kleinböhl,
Armin.Kleinboehl@jpl.nasa.gov

Citation:
Kleinböhl, A., M. Khosravi, J. Urban, T. Canty, R. J. Salawitch, G. C. Toon, H. Küllmann, and J. Notholt (2014), Constraints for the photolysis rate and the equilibrium constant of ClO-dimer from airborne and balloon-borne measurements of chlorine compounds, *J. Geophys. Res. Atmos.*, *119*, 6916–6937, doi:10.1002/2013JD021433.

Received 31 DEC 2013
Accepted 4 MAY 2014
Accepted article online 9 MAY 2014
Published online 10 JUN 2014

Constraints for the photolysis rate and the equilibrium constant of ClO-dimer from airborne and balloon-borne measurements of chlorine compounds

Armin Kleinböhl[1], Maryam Khosravi[2], Joachim Urban[2], Timothy Canty[3], Ross J. Salawitch[3,4,5], Geoffrey C. Toon[1], Harry Küllmann[6], and Justus Notholt[6]

[1] Jet Propulsion Laboratory, California Institute of Technology, Pasadena, California, USA, [2]Department of Earth and Space Science, Chalmers University of Technology, Göteborg, Sweden, [3]Department of Atmospheric and Oceanic Science, University of Maryland, College Park, Maryland, USA, [4]Department of Chemistry and Biochemistry, University of Maryland, College Park, Maryland, USA, [5]Earth System Science Interdisciplinary Center, University of Maryland, College Park, Maryland, USA, [6]Institute of Environmental Physics, University of Bremen, Bremen, Germany

Abstract We analyze measurements of ClO across the terminator taken by the Airborne Submillimeter Radiometer (ASUR) in the activated vortices of the Arctic winters of 1995/1996, 1996/1997, and 1999/2000 to evaluate the plausibility of various determinations of the ClO-dimer photolysis cross section and the rate constant controlling the thermal equilibrium between ClO-dimer and ClO. We use measured ClO during sunlit conditions to estimate total active chlorine (ClO_x). As the measurements suggest nearly full chlorine activation in winter 1999/2000, we compare ClO_x estimates based on various photolysis frequencies of ClO-dimer with total available inorganic chlorine (Cl_y), estimated from an N_2O-Cl_y correlation established by a balloon-borne MkIV interferometer measurement. Only ClO-dimer cross sections leading to the fastest photolysis frequencies in the literature (including the latest evaluation by the Jet Propulsion Laboratory) give ClO_x mixing ratios that overlap with the estimated range of available Cl_y. Slower photolysis rates lead to ClO_x values that are higher than available Cl_y. We use the ClO_x calculated from sunlit ClO measurements to estimate ClO in darkness based on different equilibrium constants, and compare it with ASUR ClO measurements before sunrise at high solar zenith angles. Calculations with equilibrium constants published in recent evaluations of the Jet Propulsion Laboratory give good agreement with observed ClO mixing ratios. Equilibrium constants leading to a higher ClO/ClO_x ratio in darkness yield ClO values that tend to exceed observed abundances. Perturbing the rates for the ClO + BrO reaction in a manner that increases OClO formation and decreases BrCl formation leads to lower ClO values calculated for twilight conditions after sunset, resulting in better agreement with ASUR measurements.

1. Introduction

Chlorine monoxide (ClO) is one of the most important species involved in polar stratospheric chemistry. In the winter polar vortex, it is formed by heterogeneous reactions of inactive chlorine species on polar stratospheric clouds [*Solomon et al.*, 1986; *McElroy et al.*, 1986] or cold sulfate aerosols [*Drdla and Müller*, 2012], followed by photolysis and the reaction with ozone. The formation of the ClO-dimer following the self-reaction of ClO leads to the catalytic destruction of ozone via the ClO-dimer cycle [*Molina and Molina*, 1987]:

$$ClO + ClO + M \underset{k_d}{\overset{k_f}{\rightleftarrows}} Cl_2O_2 + M \quad (1)$$

$$Cl_2O_2 + h\nu \xrightarrow{J} Cl + ClOO \quad (2)$$

$$ClOO + M \rightarrow Cl + O_2 + M \quad (3)$$

$$2 \cdot (Cl + O_3 \rightarrow ClO + O_2) \quad (4)$$

$$\text{net}: 2O_3 + h\nu \rightarrow 3O_2. \quad (5)$$

The ClO-dimer cycle is the most important catalytic cycle in polar ozone destruction [e.g., *World Meteorological Organization* (*WMO*), 2010; *Stratospheric Processes and their Role in Climate* (*SPARC*), 2009]. The speed at which the catalytic ozone destruction takes place is primarily determined by the photolysis rate (*J*) driving the decomposition of the ClO-dimer in reaction (2). Throughout this paper, ClO-dimer and Cl_2O_2 will be used interchangeably. The photolysis rate primarily depends on the absorption cross sections of Cl_2O_2. As it has the unit of inverse seconds, it is often called photolysis frequency; in the following these terms will be used synonymously. We note that the photolysis rates and equilibrium constants dealt with in this paper are with reference to the molecular structure ClOOCl. In addition to this isomer, other ClO-dimer isomers have been identified [*McGrath et al.*, 1988], although they are thought to be too small in abundance to affect the balance between ClO and its dimer [*SPARC*, 2009] and will not be part of this analysis.

During daytime the ClO concentration is determined by the ratio of the destruction of ClO-dimer through photolysis (reaction (2)) and thermal dissociation (back reaction in equation (1)), and the formation of ClO-dimer through the forward reaction in equation (1). In darkness, when photolysis shuts off, the ClO concentration approaches an equilibrium with its dimer [*Brune et al.*, 1990; *Vömel et al.*, 2001], which is governed by an equilibrium constant given by

$$K_{\mathrm{eq}} = \frac{k_f}{k_d}, \tag{6}$$

where k_f is the formation rate and k_d is the dissociation rate of Cl_2O_2.

Many measurements of the Cl_2O_2 absorption cross sections have been performed over the last quarter century. Most of the results from the late 1980s and 1990s were incorporated into the recommendation of the Jet Propulsion Laboratory (JPL) catalogue released in 2002 [*Sander et al.*, 2003], which also stayed unchanged in the releases of 2006 [*Sander et al.*, 2006] and 2009 [*Sander et al.*, 2009]. Using these reaction rates, chemical transport models for the polar stratosphere have been reasonably successful in simulating the observed rate of chemical loss of polar ozone in winter and spring [e.g., *Chipperfield et al.*, 2005; *Frieler et al.*, 2006; *Tripathi et al.*, 2006]. The laboratory measurement of the Cl_2O_2 cross section by *Pope et al.* [2007] caused significant new activity in this field [*SPARC*, 2009]. The *J* value for Cl_2O_2 based on the *Pope et al.* [2007] measurement would slow down modeled catalytic ozone destruction significantly, leading to major discrepancies between observed and modeled ozone loss [e.g., *von Hobe et al.*, 2007]. However, subsequent laboratory measurements by *Chen et al.* [2009] and *Papanastasiou et al.* [2009] suggest a much higher photolysis frequency for Cl_2O_2, calling the validity of the measurements by *Pope et al.* [2007] into question. The cross sections by *Papanastasiou et al.* [2009] are now recommended for use in kinetic studies in the new version of the kinetics evaluation by the Jet Propulsion Laboratory [*Sander et al.*, 2011]. The most recent laboratory measurements by *Young et al.* [2014] yielded cross sections at visible wavelengths in addition to the UV, which provides guidance for extrapolating cross sections in the UV to higher wavelengths. Figure 1 summarizes the ClO-dimer absorption cross sections published in the literature. Significant differences exist between measurements of the last 5 years and other published laboratory measurements that show lower *J* values [e.g., *Huder and DeMore*, 1995; *Pope et al.*, 2007; *von Hobe et al.*, 2009]. As the photolysis rate that controls reaction (2) tends to be the rate-limiting step in the ClO-dimer cycle, the Cl_2O_2 cross section has a significant effect on the speed at which ozone loss progresses in the polar winter stratosphere [e.g., *von Hobe et al.*, 2007].

Numerous field campaigns have been designed to provide quantitative constraints on the photochemistry of ClO and related species, given the importance of these processes for our understanding of polar ozone loss. Pioneering work was done by *Kawa et al.* [1992], who performed a comprehensive examination of the consistency of chlorine partitioning using published rate parameters. Follow-on studies examined rate parameters related to chlorine partitioning using ground-based microwave measurements [*Shindell and deZafra*, 1996], balloon-borne measurements [*Pierson et al.*, 1999], and airborne measurements of ClO [*Avallone and Toohey*, 2001]. *Vömel et al.* [2001] analyzed balloon-borne measurements of ClO at sunset to isolate the parameter k_f and showed it to be in good agreement with laboratory measurements by *Bloss et al.* [2001], which were incorporated into the JPL recommendation of 2002 [*Sander et al.*, 2003]. *Stimpfle et al.* [2004] analyzed airborne in situ measurements of ClO and its dimer and concluded that the photolysis frequencies based on cross sections recommended by *Sander et al.* [2003] were in good agreement with measurements, assuming a dimer formation rate recommended by *DeMore et al.* [2000]. *von Hobe et al.* [2007] evaluated laboratory data together with theoretical studies and field measurements and found

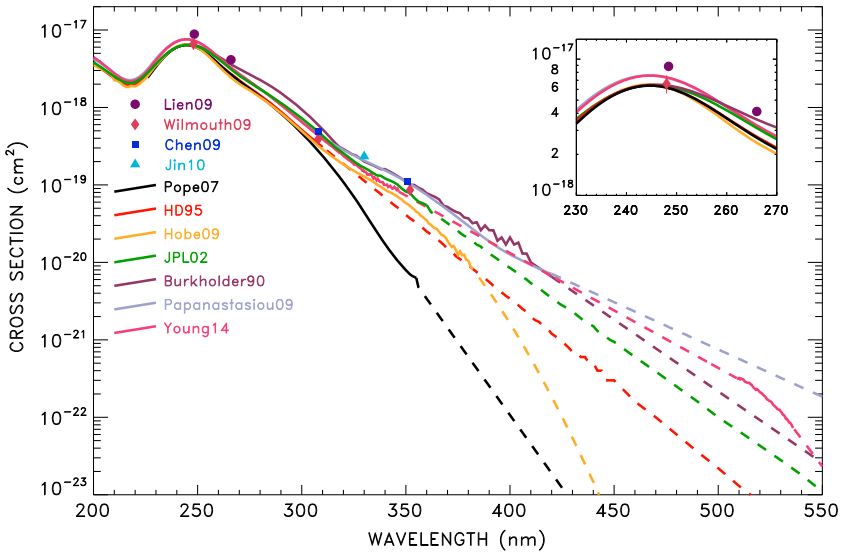

Figure 1. Absorption cross sections of ClO-dimer as published in the literature (Pope07: *Pope et al.* [2007], HD95: *Huder and DeMore* [1995], Hobe09: *von Hobe et al.* [2009], JPL02: *Sander et al.* [2003], Burkholder90: *Burkholder et al.* [1990], Papanastasiou09: *Papanastasiou et al.* [2009], Young14: *Young et al.* [2014]). Solid lines indicate the wavelength range of the measurements, while dashed lines show the extrapolation to higher wavelengths used to calculate photolysis frequencies. In the case of Young14, the dashed lines additionally show an interpolation between the measurements at UV and visible wavelengths. Symbols show absolute cross sections that were measured at isolated frequencies (Lien09: *Lien et al.* [2009], Wilmouth09: *Wilmouth et al.* [2009], Chen09: *Chen et al.* [2009], Jin10: *Jin et al.* [2010]). The inset shows the region around 248 nm in greater detail.

that photolysis cross sections between *Burkholder et al.* [1990] and the recommendation of *Sander et al.* [2006] were plausible. *Schofield et al.* [2008] and *Kremser et al.* [2011] analyzed airborne in situ measurements and ground-based microwave measurements of ClO, respectively, and suggested ratios of J/k_f up to a factor of 2 larger than recommended in *Sander et al.* [2006]. Recently, *Suminska-Ebersoldt et al.* [2012] analyzed airborne ClO in situ measurements during sunrise and suggested photolysis frequencies that are higher than the ones based on cross sections by *Pope et al.* [2007]. They found that photolysis frequencies between the ones based on cross sections by *Papanastasiou et al.* [2009] and based on *von Hobe et al.* [2009] scaled to the absolute cross-section measurement by *Lien et al.* [2009] gave reasonable agreement with their measurements.

Here we present measurements of ClO across the terminator in the polar stratosphere, taken by the Airborne SUbmillimeter Radiometer (ASUR) in the Arctic winters of 1995/1996, 1996/1997, and 1999/2000. We use ClO measurements at low solar zenith angles to estimate the total active chlorine, ClO_x, defined as

$$ClO_x = Cl + ClO + 2Cl_2O_2 + OClO + BrCl + HOCl. \quad (7)$$

As concentrations of Cl atoms, OClO, BrCl, and HOCl tend to be much smaller than of ClO and Cl_2O_2 in the winter polar lower stratosphere; for practical purposes, ClO_x will be dominated by the sum of ClO and twice its dimer. We estimate total available inorganic chlorine Cl_y using measurements of N_2O in January 2000 and a N_2O-Cl_y correlation established by a balloon measurement of the MkIV interferometer in December 1999 [*Salawitch et al.*, 2002]. We compare various ClO_x estimates for different J values of ClO-dimer, based on absorption cross sections given in JPL 2002 [*Sander et al.*, 2003], *Huder and DeMore* [1995], *von Hobe et al.* [2009], *Pope et al.* [2007] (yields lowest J value), and *Burkholder et al.* [1990] and *Papanastasiou et al.* [2009] (yield highest J values), with the Cl_y estimate. As the ClO measurements in January 2000 show nearly full chlorine activation, the comparison of ClO_x with Cl_y provides firm conclusions on the consistency between various laboratory measurements, atmospheric observations, and photochemical theory.

We give particular attention to the recent work by *Lien et al.* [2009, hereinafter Lien09], which provided an absolute cross-section measurement of ClO-dimer at 248 nm (purple dots in Figure 1). The Lien09 cross section is higher than other absolute cross-section measurements in the literature [e.g., *Burkholder et al.*, 1990; *Papanastasiou et al.*, 2009] as well as past JPL recommendations [*Sander et al.*, 2003]. Most laboratory

determinations of the absorption cross-section spectrum of ClO-dimer are relative measurements, scaled to match an absolute value around 248 nm. The higher cross section by Lien09 would lead to higher *J* values and hence a faster ClO-dimer cycle, when relative absorption cross-section spectra of ClO-dimer are scaled according to their results. We note that absolute cross-section measurements recently published by *Wilmouth et al.* [2009] are more in line with previous measurements at 248 nm (pink diamonds in Figure 1).

Another uncertainty in the behavior of ClO arises from the equilibrium constant (K_{eq}), which determines the thermally controlled partitioning of ClO and its dimer in reaction (1), leading to uncertainties in the amount of ClO present in twilight and nighttime conditions. Estimates of the equilibrium constant from laboratory measurements and atmospheric ClO measurements differ. The equilibrium constant measured by *Cox and Hayman* [1988] is in very good agreement with atmospheric measurements by *Avallone and Toohey* [2001] at stratospheric temperatures [*von Hobe et al.*, 2007], while values of K_{eq} published in recent JPL recommendations [*Sander et al.*, 2006, 2009] are higher. Atmospheric measurements by *von Hobe et al.* [2005] yielded a much lower equilibrium constant at stratospheric temperatures; however, *von Hobe et al.* [2007] note that equilibrium might not have been established in these measurements. Nighttime observations of ClO and its dimer by *Stimpfle et al.* [2004] using airborne in situ instrumentation show good agreement with equilibrium constants by *Cox and Hayman* [1988] and *Avallone and Toohey* [2001], while nighttime ClO observations by *Suminska-Ebersoldt et al.* [2012] require the equilibrium constant based on *Plenge et al.* [2005] to yield ClO_x amounts that are below the total available inorganic chlorine. Satellite measurements of nighttime ClO from the Sub-Millimetre Radiometer instrument on the Odin satellite were found to be in agreement with model calculations using K_{eq} from *von Hobe et al.* [2005] at temperatures around 210 K and from *Cox and Hayman* [1988] for lower temperatures, while K_{eq} from the JPL recommendation [*DeMore et al.*, 2000] leads to an underestimate of observed nighttime ClO [*Berthet et al.*, 2005]. ClO measurements from the Microwave Limb Sounder on EOS-Aura were used to analyze the temperature dependence of K_{eq} [*Santee et al.*, 2010]. Good agreement is achieved with the formulation of *Avallone and Toohey* [2001] but agreement is still within the error bars when the JPL recommendations by *Sander et al.* [2006, 2009] are considered, while K_{eq} from *von Hobe et al.* [2005] leads to higher nighttime ClO than observed.

We use a one-dimensional photochemical model to calculate the variation of ClO with solar zenith angle (SZA) across the day-night and night-day transitions for the different photolysis cross sections and equilibrium constants. We compare the calculations with the ClO measurements across the terminator and draw conclusions on the plausibility of various determinations of K_{eq}.

The day-night transition of ClO is to a large extent influenced by the formation rate of ClO-dimer (forward reaction in equation (1)). This termolecular reaction can be parameterized as

$$k_f = \frac{k_0[M] \cdot k_\infty}{k_0[M] + k_\infty} \cdot 0.6^{(1+(lg(k_0[M]/k_\infty))^2)^{-1}}, \tag{8}$$

where $[M]$ is the molecular air density. *Sander et al.* [2003] give the low-pressure limit as $k_0 = 1.6 \cdot 10^{-32}(T/300)^{-4.5} \frac{cm^6}{molecules^2 \cdot s}$ and the high-pressure limit as $k_\infty = 2 \cdot 10^{-12}(T/300)^{-2.4} \frac{cm^3}{molecules \cdot s}$, where T is the temperature in K. Subsequent revisions to this reference have only provided updates to the high-pressure limit, which has only a minor influence on chemistry in the stratosphere, so all analyses in the following are performed with reference to the ClO-dimer formation rate of *Sander et al.* [2003].

The behavior of ClO across the day-night transition is also influenced by the reaction between ClO and BrO. This reaction has three branches [*Friedl and Sander*, 1989], yielding the products OClO, ClOO, and BrCl, respectively,

$$ClO + BrO \rightarrow Br + OClO \tag{9}$$

$$\rightarrow Br + ClOO \tag{10}$$

$$\rightarrow BrCl + O_2. \tag{11}$$

The branching ratios of the ClO + BrO reaction are uncertain and have been previously examined based on measurements of OClO obtained during twilight [*Salawitch et al.*, 1988] and nighttime [*Canty et al.*, 2005]. The decrease of ClO versus SZA during the day-night transition is sensitive to the ClO-dimer formation rate and the rate of reaction of ClO with BrO, and uncertainties in the various branches of the ClO + BrO reaction will lead to different behavior. We will study this influence using the one-dimensional model in comparison with the ASUR ClO measurements.

The paper is structured in the following way: In section 2, we describe the instruments and measurements used in this study. In particular, we introduce the Airborne SUbmillimeter Radiometer (ASUR) and its measurement characteristics, as well as its measurements of ClO and other gases relevant to this study in section 2.1. We describe the MkIV balloon-borne Fourier transform interferometer and its measurements in section 2.2. This section also describes the derivation of Cl_y from the MkIV measurements. Section 3 deals with the model simulations employed to interpret the measurements. In section 3.1, we derive ClO_x from ASUR ClO measurements at low solar zenith angles using a photochemical model in diurnal steady state [*Stimpfle et al.*, 2004; *Canty et al.*, 2005] and compare it with available Cl_y to draw conclusions on the plausibility of various photolysis frequencies. We introduce model simulations of the diurnal variation of ClO with the MISU-1D model [*Jonsson*, 2006; *Khosravi et al.*, 2013] in section 3.2. These simulations are used to interpret ASUR ClO measurement sequences across the sunrise terminator and draw conclusions on the plausibility of various formulations of K_{eq} in section 3.3. Section 3.4 discusses calculations with the same model to evaluate the ClO-BrO cycle based on an ASUR ClO measurement sequence across the sunset terminator. We summarize our conclusions in section 4.

2. Measurements

2.1. Airborne Submillimeter Measurements

The key measurements used in this study were obtained by the Airborne SUbmillimeter Radiometer (ASUR) [*von König et al.*, 2000, and references therein]. The instrument uses a liquid helium cooled detector to measure the emission of submillimeter radiation in a frequency range between 604.3 and 662.3 GHz. Before 1999, the frequency range was 624–654 GHz. An acousto-optical spectrometer is used for the acquisition of spectra. A filter bank was also available until 1997. The ASUR instrument is operated on board an aircraft flying at 10–12 km altitude to avoid signal absorption by tropospheric water vapor. Observations were performed through a high-density polyethylene window on the starboard side of the aircraft. Atmospheric measurements were taken at a stabilized elevation angle of 12°; hence, the location of the origin of the stratospheric signal is offset from the flight track. For signals originating 10 km above the aircraft, the horizontal offset is about 47 km perpendicular to the flight track. An atmospheric measurement is bracketed by measurements of calibration loads at ambient and liquid nitrogen temperatures. This measurement cycle takes about 6 s to complete.

By analyzing the spectrally resolved pressure broadened emission lines with optimal estimation [*Rodgers*, 2000], vertical profiles of the volume mixing ratio (VMR) of ClO, HCl, ozone, N_2O, and other trace gases can be retrieved over an altitude range of about 15–40 km with a typical vertical resolution of 6–10 km in the lower stratosphere. For the retrieval, spectra from several measurement cycles are integrated to improve the signal-to-noise ratio. This integration time determines the horizontal resolution of the measurement along the flight track. With an aircraft speed of about 700 km h^{-1}, ClO measurements have horizontal resolutions of ~50 km, while for N_2O horizontal resolutions of ~25 km and for HCl and ozone horizontal resolutions of less than 20 km are achieved.

The accuracy of the ASUR measurement is composed of the statistical error, which is mainly determined by the noise in the measurement and the quality of the fit, and by systematic error sources. Estimates of the systematic error include contributions from uncertainties in the observation angle, the actual flight altitude, and uncertainties in the calibration system, such as the reflectivity of the cold calibration load. The systematic error also includes uncertainties in the model parameters used for the inversion, e.g., spectroscopic parameters like line intensities and pressure broadening coefficients, meteorological profiles, and the parameterization of continuum absorption [*von König*, 2001]. Adding these sources quadratically and taking the statistical error into account results in an accuracy of 10% or 0.15 ppb, whichever is higher, for a typical ClO profile in an altitude range between 15 and 40 km. For HCl, the accuracy is approximately 15% or 0.1 ppb, whichever is higher, while for N_2O, these values are 15% and 30 ppb [*von König*, 2001; *Kleinböhl et al.*, 2002]. These uncertainty estimates, as well as all others in this paper, are considered 1σ errors.

For this study new ClO retrievals were performed such that all retrievals are based on a consistent set of input parameters. Figure 2 (left) shows the a priori profile and the a priori error used in the new set of retrievals. The a priori error is a compromise between the one used in the original retrievals from the SAGE-III Ozone Loss and Validation Experiment (SOLVE) campaign in 1999/2000 [*Bremer et al.*, 2002], and the one used for the analyses in the 1990s [*Urban*, 1998]. The resulting averaging kernels for a typical ClO retrieval

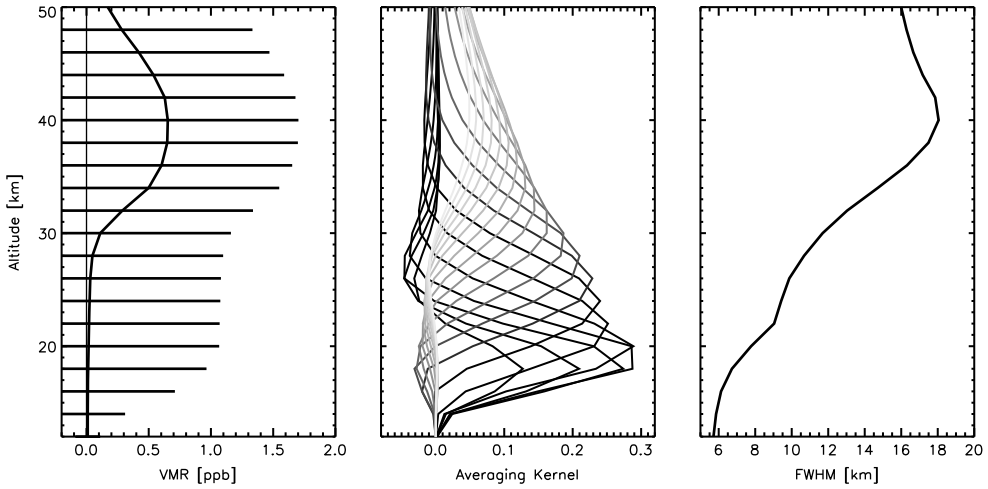

Figure 2. (left) ClO a priori profile and a priori error (marked as error bars) used in the ASUR retrieval. (middle) ClO averaging kernels resulting from the ASUR retrieval. Kernels at higher altitude levels are drawn in successively lighter gray. (right) Full width at half maximum (FWHM) of the averaging kernels.

are shown in Figure 2 (middle). The kernel centered at 20 km altitude has a full width at half maximum of about 7–8 km (Figure 2 (right)).

Table 1 gives an overview on the research flights considered in this paper, during which the diurnal variation of ClO was measured by the ASUR instrument. These flights took place during three different Arctic winters. During two of the flights transitions from night to day were observed, while during the other flight a transition from day to night was measured. A fourth flight that took place on 25 February 1996 is not considered because it seemed to have encountered quite variable conditions of activated chlorine [*Urban*, 1998].

All flights were performed inside the polar vortex and encountered perturbed chlorine chemistry. The flights in 1996 and 1997 were short flights on board the German research aircraft Falcon. These flights were designed to measure the diurnal variation of ClO [*Urban*, 1998]. They were conducted west of Kiruna, Sweden, and roughly followed a circle of constant latitude. On one leg of a flight, ClO was measured almost continuously over the terminator, while on the opposite leg, other species were measured, interspersed with occasional measurements of ClO. For the flight in 1997, the track was optimized based on meteorological wind analyses to allow nearly the same air masses to be measured on both flight legs [*Eyring*, 1999]. The flight in 2000 was performed on board the NASA DC-8 research aircraft and had multiple objectives. Continuous ClO measurements were made along a profile of nearly constant longitude, capturing a night-day transition. Other species, in particular HCl and N_2O, were measured by ASUR in the vicinity of the ClO observations.

Figure 3 shows the retrieved ClO profiles from ASUR measurements versus SZA along each flight track across the terminator, together with the location and equivalent latitude of each measurement. Equivalent latitude is a measure of the area enclosed by a line of constant potential vorticity, where this area is assumed to be circular and centered on the pole.

Table 1. Key Parameters of the ASUR Flights Where ClO Across the Terminator was Measured

Campaign	Date of Flight	Location[a]	Aircraft	Type of Transition
GOME validation	2 Mar 1996	70.3°N,16.9°E	DLR Falcon	Night-Day
ILAS validation	25 Feb 1997	69.7°N,3.8°E	DLR Falcon	Day-Night
SOLVE	23 Jan 2000	69.0°N,16.8°E	NASA DC-8	Night-Day

[a]Location gives the approximate location where a solar zenith angle of 90° was reached.

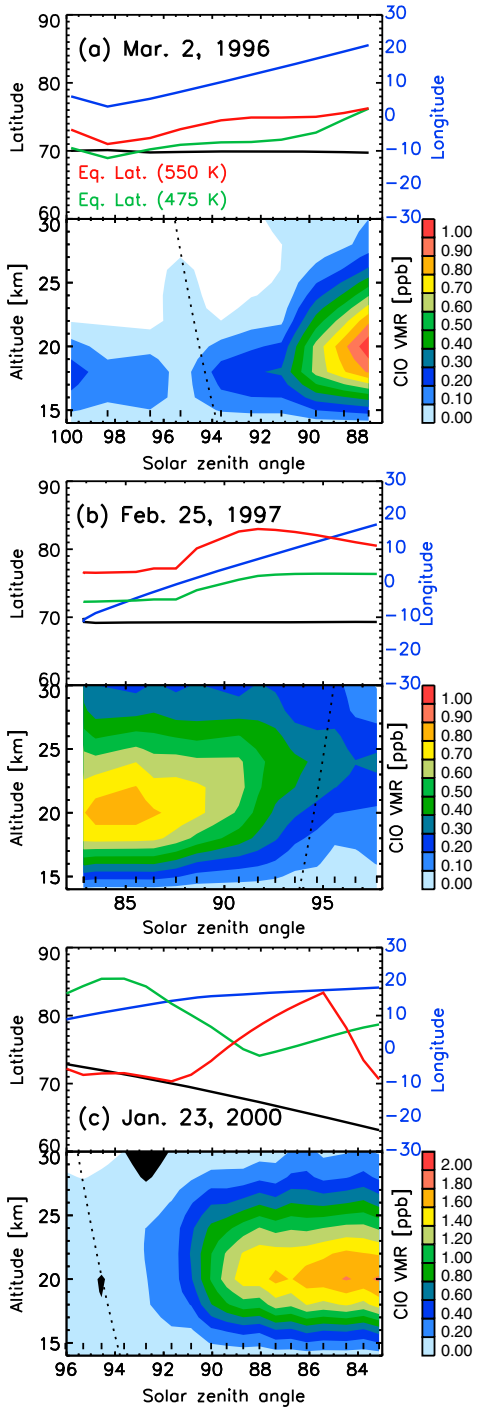

Figure 3. Color-contoured ClO volume mixing ratio profiles retrieved from ASUR measurements on flights across the terminator on (a) 2 March 1996, (b) 25 February 1997, and (c) 23 January 2000. Note that the color scale in Figure 3c is different from the one in Figures 3a and 3b. Black dashes on the contour plot show the locations of the actual measurements. The dotted line indicates the astronomical terminator. The line plots show latitude (black), equivalent latitude at 475 K (green), and equivalent latitude at 550 K (red) of each measurement with reference to the left *y* axis, as well as the longitude (blue) of each measurement with reference to the right *y* axis.

In March 1996, a sunrise flight was performed. The equivalent latitudes both at 475 K and 550 K potential temperature (corresponding to about 19 and 22 km altitude) stay between 70° and 75° throughout the flight. The maximum ClO observed was about 1.1 ppb at 87.5° SZA at 20 km altitude.

The February 1997 flight was a sunset flight. Homogeneous conditions in terms of equivalent latitude were recorded for low solar zenith angles, while equivalent latitudes increased slightly toward higher solar zenith angles. The route for this flight was planned such that the outbound leg measured roughly the same air masses at nearly constant SZAs as the inbound leg over the terminator. Chlorine activation showed little inhomogeneity along this outbound leg, with ClO mixing ratios varying only by about ±5% (not shown). These mixing ratios are consistent with vortex averages of ClO observed by *Santee et al.* [1997], who also reported large areas of activated ClO to be still present at this season. Maximum ClO values were observed to be around 0.85 ppb at 20 km between 83° and 86° SZA. Note that the ClO VMR across the terminator changes more slowly in sunset conditions compared to sunrise conditions.

The flight in January 2000 again was a sunrise flight. Maximum ClO values of about 1.8 ppb were observed at 20 km at SZAs of 83°–85°. Figure 4 shows a retrieved HCl profile in the vicinity of the ClO measurements. HCl mixing ratios are essentially zero in a region around 18–20 km altitude. High ClO mixing ratios were measured together with very low HCl mixing ratios throughout the vortex in mid- to late-January 2000 [*Bremer et al.*, 2002]. This suggests that conditions inside the vortex were close to full activation. This is supported by in situ measurements of $ClNO_3$ from the ER-2 high-altitude aircraft. $ClNO_3$ mixing ratios at lower stratospheric altitudes inside the vortex were reported to be below the detection limit of 20 parts per trillion (ppt) for flights conducted in mid- to late-January 2000 (including a flight on 23 January 2000) [*Wilmouth et al.*, 2006]. Equivalent latitudes along the ClO measurement sequence by ASUR are somewhat variable. However, the lowest equivalent latitude during this measurement sequence was 70°, well inside the Arctic vortex in January 2000 [*Kleinböhl et al.*, 2002]. This suggests that the flight on 23 January 2000 is suitable for a meaningful analysis despite variations in equivalent latitude.

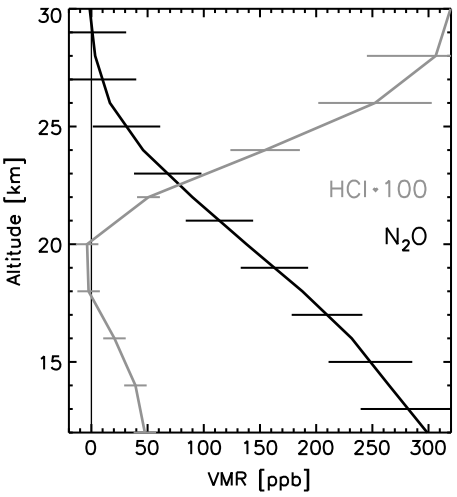

Figure 4. Profiles of N_2O at 68.2°N, 17.1°E, and of HCl at 67.2°N, 20.0°E, retrieved from ASUR measurements on 23 January 2000. Error bars give the estimated accuracy.

2.2. Balloon-Borne FTIR Measurements

Ancillary measurements that constrain the total available inorganic chlorine (Cl_y) in the lower stratosphere were performed by the JPL MkIV Fourier transform interferometer [*Toon*, 1991]. The MkIV covers a spectral range between 650 and 5650 cm^{-1} with a spectral resolution of ~0.01 cm^{-1}. It is operated on a high-altitude balloon and views the Sun through the atmospheric limb at sunset or sunrise. Due to the long viewing path through the atmosphere, MkIV provides high sensitivity to more than 30 trace gases, among them the Cl_y constituents HCl, $ClNO_3$, ClO, and HOCl, as well as stratospheric tracers like N_2O and CH_4.

On 3 December 1999, MkIV performed a sunset flight from Esrange, Sweden (67.9°N, 21.1°E) [*Coffey et al.*, 2002; *Salawitch et al.*, 2002]. This flight occurred at the onset of the SOLVE winter and measured largely unprocessed air inside the polar vortex, hence giving a good constraint on the available inorganic chlorine. Another MkIV flight from Esrange was performed on 15 March 2000 at sunrise during the breakup of the vortex. Figure 5 shows retrievals of N_2O, HCl, $ClNO_3$, ClO, and HOCl from the December 1999 flight. Error bars give the accuracy for each individual species, primarily driven by uncertainties in the spectroscopic parameters used for retrieval. Based on the measured ClO during the balloon flight, we calculate the mixing ratio of ClO-dimer (using photolysis cross sections from [*Sander et al.*, 2003]). Chlorine activation was minimal during this time, with a maximum value of 0.3 ppb retrieved between 20 and 25 km altitude. The contribution of ClO-dimer to overall Cl_y is very small. Nevertheless, for the sake of completeness, we have defined Cl_y as

$$Cl_y = HCl + ClNO_3 + ClO + HOCl + 2Cl_2O_2. \quad (12)$$

This Cl_y profile is also given in Figure 5 (middle) together with its accuracy, derived from the accuracy of the individual Cl_y constituents. The maximum value for Cl_y is 3.67 ± 0.18 ppb between 25 and 30 km altitude. This is consistent with Cl_y estimated from ground-based measurements of organic chlorine in the troposphere, if a stratospheric age of air of 5–6 years is assumed [*Montzka et al.*, 1999; *O'Doherty et al.*, 2004].

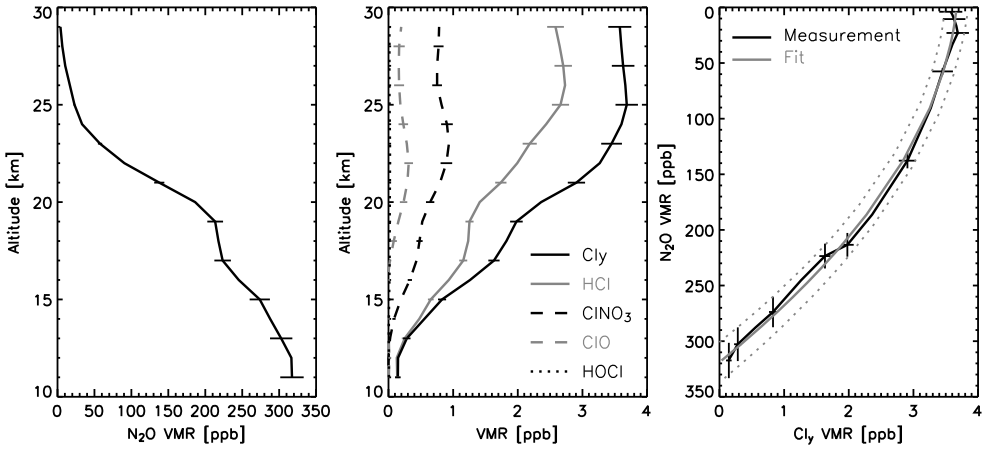

Figure 5. (left) N_2O profile measured by the MkIV instrument during the balloon flight on 3 December 1999. (middle) MkIV measurements of HCl, $ClNO_3$, ClO, and HOCl from the same balloon flight, and the derived Cl_y. (right) Cl_y based on the MkIV measurements plotted versus N_2O (black), and second-order polynomial fit of the N_2O-Cl_y correlation (solid gray) and its error (dotted gray).

Figure 5 (right) shows the N_2O-Cl_y correlation based on the N_2O profile measured by MkIV on the same balloon flight. Uncertainties in the correlation (crosses in Figure 5) are largely driven by the accuracy of N_2O in the lower stratosphere, and by the accuracy of the Cl_y at higher altitudes. Fitting the correlation with a second-order polynomial yields

$$VMR_{Cl_y} = 3.668 \cdot 10^{-9} - 0.001827 \cdot VMR_{N_2O} - 30343 \cdot VMR^2_{N_2O}, \quad (13)$$

where both Cl_y and N_2O are given in units of 1. The correlation is valid between 4 and 317 ppb N_2O. The fit is shown in Figure 5 (right) together with its uncertainty, derived as a maximum error from the individual accuracies in N_2O and Cl_y.

3. Comparisons With Photochemical Model Calculations

3.1. Comparison of ClO_x With Cl_y

To quantify the plausibility of various photolysis frequencies based on our current understanding of chlorine chemistry, we compare ClO_x inside the polar vortex with the estimate of Cl_y derived in the previous section. For the calculation of ClO_x profiles, we use the photochemical model given in *Stimpfle et al.* [2004] and *Canty et al.* [2005]. It simultaneously calculates the 24 h diurnal variation, at 15 min intervals, of ClO, ClOOCl, BrO, BrCl, and OClO using a Newton-Raphson iterative method. The model operates in a diurnal steady state; that is, production and loss rates of these species are forced to be equal when integrated over the full 24 h time period. These simulations are constrained to latitude, longitude, pressure, temperature, SZA and declination, time of day, and ClO at the time and location of the ASUR observations. A profile of BrO_x (BrO_x = Br + BrO + BrCl), calculated using balloon-borne differential optical absorption spectroscopy observations of BrO over Kiruna, Sweden, on 18 February 2000 [*Dorf et al.*, 2006] and shown in Figure S1 of the supporting information, is used to determine the relative abundance of reactive bromine species. Both ClO_x and BrO_x are held constant. NO_y species, such as $ClNO_3$, are not considered (see *Canty et al.* [2005, Appendix A]). The calculation of photolysis frequencies is carried out using a radiative transfer model that includes Rayleigh scattering. In this code, photolysis does not shut down when SZA$>$ 90°, which allows for the simulation of the temporal variation of the chemistry across the terminator. The ozone profiles used as input for the calculation of the optical depth in the atmosphere are shown in Figure S1 of the supporting information. They were taken from ozone sonde measurements over Sodankylä, Finland, up to ∼30 km [*Kivi et al.*, 2007], and extended to higher altitudes by ASUR ozone measurements.

As the formation rate of ClO-dimer depends quadratically on the concentration of ClO (reaction (1)) care must be taken concerning the limited altitude resolution of the ASUR measurement. A deviation of the true structure of a profile from the structure obtained by the retrieval might introduce errors in the calculated ClO_x. Figure 6 shows the ClO profile retrieved from the measurement at the lowest SZA of the measurement sequence from 23 January 2000 (Figure 3). These ClO values were quite common in the sunlit part of the Arctic vortex in January 2000 [*Bremer et al.*, 2002; *Rex et al.*, 2002]. To assess the impact of the averaging kernels, we specify a profile on a 1 km grid and test whether it agrees with the retrieved ClO after applying the averaging kernels. The dashed lines in Figure 6 give two examples of such profiles. One example is a 1 km resolution profile of ClO with a peak at the same altitude as the retrieved one, only the peak is narrower in altitude and has a higher maximum VMR (profile (a) in Figure 6). If the peak VMR of this profile was significantly larger, then the convolved profile would not be in agreement with the profile retrieved from the ASUR measurement. Another example is a profile with a peak of a similar magnitude as the retrieved ClO profile but at a higher altitude, with a steeper slope above the peak (profile (b) in Figure 6). If the peak of this profile were to be shifted to higher altitudes, the convolved profile would no longer agree with the measurement. Both assumed high-resolution ClO profiles fit the retrieved ClO profile within its precision (error bars in Figure 6) after application of the ASUR averaging kernels (dotted lines). Figure 6 (right) shows profiles of ClO_x, calculated from these high-resolution ClO profiles using photolysis frequencies based on ClO-dimer absorption cross sections recommended in *Sander et al.* [2003]. We note that other ClO profiles could also fit the profile shape measured by ASUR when convolved with the averaging kernels. Sensitivity studies show that profiles with peaks at lower altitudes or with a more complicated structure tend to result in higher ClO_x mixing ratios at altitudes below 20 km, which makes them less probable given further considerations presented below. Profiles (a) and (b) can be considered as bracketing a range of plausible profiles that explain the ASUR observations at the 1σ level.

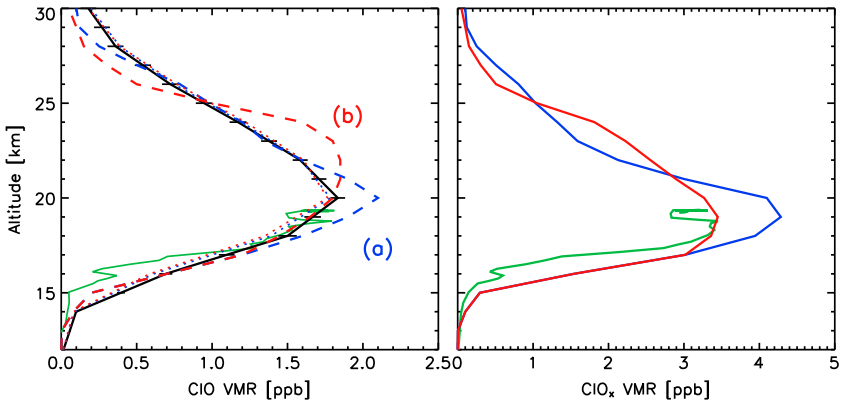

Figure 6. (left) Retrieved ClO profile from ASUR measurement on 23 January 2000 at 63.2°N, 19.1°E, at an SZA of 83.1° (black). The error bars indicate the precision. Also shown are plausible profiles of higher resolution (profiles (a) and (b), colored dashed lines, see text for description) that yield the retrieved ClO profile within the precision when convolved with ASUR the averaging kernels (colored dotted lines). The green line gives ClO from an in situ measurement on board the ER-2 from the same day in the vicinity of the ASUR measurement. (right) ClO_x calculated from the ClO profiles (a) (blue) and (b) (red) as well as the ER-2 ClO profile (green) using photolysis cross sections from *Sander et al.* [2003].

To further check the realism of these assumptions, we compare our profiles with in situ measurements of ClO from the ER-2 high-altitude aircraft [*Stimpfle et al.*, 2004]. The ER-2 also performed a flight on 23 January 2000, during which it conducted a descent that started roughly an hour after the high-Sun ClO measurement by ASUR on that day, and was located within 2° latitude and longitude of that measurement [*Stimpfle et al.*, 2004]. The ClO profile measured by the ER-2 during descent, for SZAs between 80.7° and 84.1°, is shown as the green line in Figure 6. While showing a slightly steeper slope at low altitudes, the ClO VMRs measured by the in situ instrument between ~17 and 20 km are very similar to the input profiles assumed for the simulation of the ASUR measurements, in particular profile (b). The ER-2 profile of ClO shows that there was little small-scale variability with respect to altitude in the vicinity of the ASUR measurement. We calculated ClO_x from the ER-2 profile of ClO in the same manner as done for ASUR ClO. The result is included in Figure 6. The ClO_x calculated from the ER-2 measurement is slightly lower than from the ASUR profile because the ER-2 measurement was located slightly south of the ASUR measurement, and hence experienced a lower SZA at ~17–20 km altitude. However, the result is still very close to the ClO_x calculated from profile (b). We note that profile (b) also qualitatively resembles the shape of several ClO profiles measured in situ from different balloon-borne platforms during the winter 1999/2000 [*Vömel et al.*, 2001; *Vogel et al.*, 2002; *Rex et al.*, 2002], so it is likely to be a realistic representation of the vertical distribution of ClO.

The Cl_y profile representative for the time and location of the ASUR measurements on 23 January 2000 is calculated using the ASUR N_2O profile shown in Figure 4 and the N_2O-Cl_y correlation given by equation (13). Although N_2O is retrieved with an altitude resolution comparable to ClO, the slope in a typical N_2O profile can be much better reproduced than a peaked profile. Consequently, the retrieved N_2O is expected to be a good estimate of the actual N_2O distribution in the lower stratosphere [*Greenblatt et al.*, 2002]. The accuracy in the Cl_y profile is found by combining the uncertainty in the correlation itself (see Figure 5 (right)) and the accuracy in the ASUR N_2O profile. This results in Cl_y values of $3.67^{+0.18}_{-0.26}$ ppb at 30 km and $2.84^{+0.46}_{-0.56}$ ppb at 20 km altitude.

We use the high-resolution ClO profile estimates given in Figure 6 and the BrO_x profile given in Figure S1 of the supporting information to calculate Cl_2O_2 using the aforementioned photochemical model. Subsequently, ClO_x is calculated using equation (7). Estimates of ClO_x are provided for photolysis cross sections of Cl_2O_2 given by *Young et al.* [2014], *Papanastasiou et al.* [2009], *Burkholder et al.* [1990], JPL 2002 [*Sander et al.*, 2003], *von Hobe et al.* [2009], *Huder and DeMore* [1995], and *Pope et al.* [2007]. The photolysis frequencies resulting from these cross sections are given in Table 2 for the conditions of the ASUR high-sun measurement on 23 January 2000. The value of K_{eq} is taken from JPL 2009 [*Sander et al.*, 2009], all other relevant rate constants are from JPL 2002 [*Sander et al.*, 2003]. To estimate an accuracy of the Cl_2O_2, calculations have been performed with ClO VMRs enhanced and reduced by 10%, based on the accuracy of the ASUR ClO measurement. The accuracy of the resulting ClO_x, shown by the error bars in Figure 7, is based on these estimates.

Table 2. Photolysis Frequencies of Cl_2O_2 Given in s^{-1} as Calculated for the ASUR Measurement on 23 January 2000, at an SZA of 83.1° for 18 km and 20 km Altitude, Respectively

Data Set No.	J (18 km)	J (20 km)	J (18 km) Scaled to Lien09	J (20 km) Scaled to Lien09	Reference[a]
1	$1.04 \cdot 10^{-3}$	$1.15 \cdot 10^{-3}$	$1.26 \cdot 10^{-3}$	$1.4 \cdot 10^{-3}$	*Young et al.* [2014]
2	$1.37 \cdot 10^{-3}$	$1.51 \cdot 10^{-3}$	$1.67 \cdot 10^{-3}$	$1.84 \cdot 10^{-3}$	*Papanastasiou et al.* [2009]
3	$1.39 \cdot 10^{-3}$	$1.53 \cdot 10^{-3}$	$1.92 \cdot 10^{-3}$	$2.12 \cdot 10^{-3}$	*Burkholder et al.* [1990]
4	$9.78 \cdot 10^{-4}$	$1.09 \cdot 10^{-3}$	$1.38 \cdot 10^{-3}$	$1.54 \cdot 10^{-3}$	*Sander et al.* [2003]
5	$6.19 \cdot 10^{-4}$	$6.98 \cdot 10^{-4}$	$9.06 \cdot 10^{-4}$	$1.02 \cdot 10^{-3}$	*von Hobe et al.* [2009]
6	$5.48 \cdot 10^{-4}$	$6.21 \cdot 10^{-4}$	$7.9 \cdot 10^{-4}$	$8.95 \cdot 10^{-4}$	*Huder and DeMore* [1995]
7	$1.62 \cdot 10^{-4}$	$1.96 \cdot 10^{-4}$	$2.34 \cdot 10^{-4}$	$2.82 \cdot 10^{-4}$	*Pope et al.* [2007]

[a]Results are presented for the original cross sections given in the references, and with the cross sections scaled to the measurement by *Lien et al.* [2009] (see text).

The impact of various Cl_2O_2 photolysis cross sections on calculated ClO_x is represented by the different symbols in Figure 7, based on ASUR ClO for the flight of 23 January 2000 for altitudes of (top) 20 km and (bottom) 18 km. Below 18 km, ASUR starts to lose sensitivity; above 20 km, ClO_x starts to decrease (Figure 6) while Cl_y is still increasing (Figure 5), leading to less meaningful comparisons. Given the original cross sections (diamonds in Figure 7) the only estimates of ClO_x that overlap, within respective uncertainties, the estimate for Cl_y are those based on the cross sections published by *Papanastasiou et al.* [2009] and *Burkholder et al.* [1990] for profiles (a) and (b). ClO_x based on JPL 2002 cross sections [*Sander et al.*, 2003] as well as based on cross sections by *Young et al.* [2014] give overlap within the accuracies when profile (b) of Figure 6 is considered. The ClO_x values found using these cross sections and ClO profile (a) are higher than our estimate of Cl_y. We note that the original cross-section spectra published by *Young et al.* [2014], which were used in the calculations of Figure 7, are scaled to the absolute cross sections by *Papanastasiou et al.* [2009] at 248 nm because they were made after the *Papanastasiou et al.* [2009] cross sections were adopted by *Sander et al.* [2011]. The ClO_x based on *Young et al.* [2014] is still closer to the result based on *Sander et al.* [2003] than to the one based on *Papanastasiou et al.* [2009], likely because the *Young et al.* [2014] cross sections closely follow the ones by *Sander et al.* [2003] in the near-UV (Figure 1). Cross sections by *von Hobe et al.* [2009] and *Huder and DeMore* [1995] result in values of ClO_x that are much higher than available Cl_y. The ClO_x values calculated with the *Pope et al.* [2007] cross sections have to be considered unrealistically

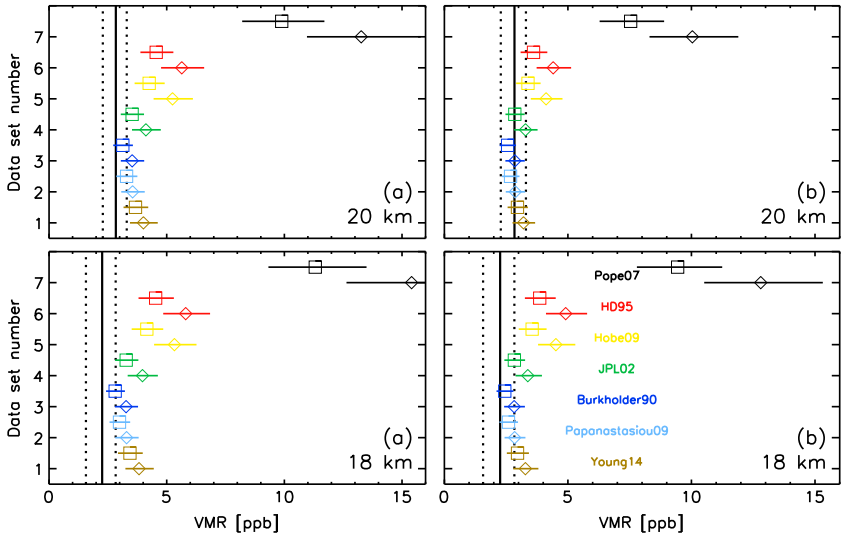

Figure 7. Comparison of ClO_x (colored symbols) with available Cl_y (vertical solid black lines with dotted lines giving the accuracies) for (bottom) 18 km and (top) 20 km altitude. ClO_x was calculated based on the input ClO profiles (left) (a) and (right) (b) from Figure 6 using different cross sections according to the data set number (1: *Young et al.* [2014], 2: *Papanastasiou et al.* [2009], 3: *Burkholder et al.* [1990], 4: JPL02 [*Sander et al.*, 2003], 5: *von Hobe et al.* [2009], 6: *Huder and DeMore* [1995], and 7: *Pope et al.* [2007]). ClO_x values marked as diamonds were calculated using the original cross sections, while for the ones marked by squares, the cross sections were scaled to the value of Lien09.

large given our present understanding of chlorine chemistry, which is in line with results of previous studies [e.g., *Schofield et al.*, 2008; *Kremser et al.*, 2011; *Suminska-Ebersoldt et al.*, 2012].

The squares in Figure 7 show estimates of ClO_x found using the aforementioned cross sections, scaled linearly to the absolute cross section by Lien09. This scaling involves multiplying various cross sections by a specific constant, multiplicative factor such that the scaled cross section matches the measurement of Lien09 at 248 nm (Figure 1). Although *Papanastasiou et al.* [2009] and *Burkholder et al.* [1990] provide absolute measurements, we report values of ClO_x using their cross sections scaled to Lien09 for the sake of completeness. The values of ClO_x found using cross sections scaled to Lien09 are lower than when calculated with the original cross sections, which brings ClO_x closer to estimated Cl_y for most cases considered in Figure 7. Scaling the JPL 2002 cross sections to Lien09 reduces the calculated ClO_x such that it now overlaps with estimated Cl_y within the various uncertainties. The ClO_x values based on the *Young et al.* [2014] cross sections scaled to Lien09 are within the available Cl_y range if profile (b) is considered but still slightly higher than available Cl_y at 18 km if profile (a) is considered. Cross sections reported by *von Hobe et al.* [2009] and *Huder and DeMore* [1995], when scaled to Lien09, produce values of ClO_x that are still higher than the Cl_y estimate for most cases considered in Figure 7. This suggests that scaling these cross sections to Lien09 is not sufficient to reconcile these laboratory measurements with observed atmospheric composition, given our present understanding of ClO_x photochemistry. This is in contrast to the reasonably good agreement between observed and calculated ClO at sunrise by *Suminska-Ebersoldt et al.* [2012] with cross sections by *von Hobe et al.* [2009] scaled to Lien09. The scaling of the *Pope et al.* [2007] cross sections still produces much more ClO_x than available Cl_y.

3.2. Study of ClO Diurnal Variations

To evaluate the diurnal variation of ClO in detail, model simulations were performed with the MISU-1D photochemical model [*Jonsson*, 2006; *Khosravi et al.*, 2013]. MISU-1D is a 1-D photochemical model that uses detailed radiative transfer calculations in the UV and visible region, in which multiple scattering and albedo effects are incorporated [*Meier et al.*, 1982]. The sphericity of the Earth is taken into account, which allows for nonzero transmitted flux at SZA> 90°. The input solar flux for the calculation of photolysis rates is adopted from the *WMO* [1986] reference spectrum. The Earth-Sun distance was corrected for seasonal variations according to *Madronich* [1993]. Ozone absorption cross sections and oxygen absorption cross sections in the Schumann-Runge bands are in accordance with *WMO* [1986] recommendations and the *Koppers and Murtagh* [1996] algorithm, respectively. The Herzberg continuum is taken from *Nicolet and Kennes* [1986]. A system of stiff ordinary differential equations is solved with a variable order method. The algorithm solves the time evolution of each species present in the reaction scheme. Most of the calculations of ClO reported below using the MISU-1D model were repeated with the model described in section 3.1; nearly identical results were found and our conclusions are robust regardless of model choice.

Chemical loss of polar ozone under twilight conditions is controlled almost exclusively by ClO_x and BrO_x chemistry; therefore, chlorine and bromine cycles are considered for this analysis. Since all of the chlorine and bromine in the model is considered to be in the active form, the model is initialized with ClO_x and BrO_x by setting ClO to ClO_x and BrO to BrO_x, all other species are initialized to be zero. The model runs for 5 days to converge to a solution, after which the concentration of species changes insignificantly between subsequent days. The photolysis frequencies of ClO-dimer (reaction (2)) and K_{eq} (reaction (1)) primarily determine the relative abundances of ClO and Cl_2O_2 in the model, particularly during mid-day and completely dark conditions. The full 24 h diurnal cycle with a variable Sun position is simulated with the calculation of *J* values updated at each time step in the solver (every 3 min). The model is also constrained using meteorological analyses of temperature and pressure along the flight track.

The ozone profiles and the BrO_x profile used as input for the calculations are the same as in section 3.1 and shown in Figure S1 of the supporting information. Ozone concentrations are fixed throughout the model run. The simulations were performed for conditions of the locations of the measurements (Table 1). The measurement flights in March 1996 and February 1997 were carried out along almost constant latitudes (Figure 3). The corresponding model simulations were conducted for a mean latitude of 69.8°N and 69.3°N, respectively. The January 2000 flight was carried out across a latitudinal range from 71.1°N to 63.1°N. The simulations for this flight were conducted at the latitude of each individual ClO profile and then reassembled to construct the observed diurnal variation of ClO.

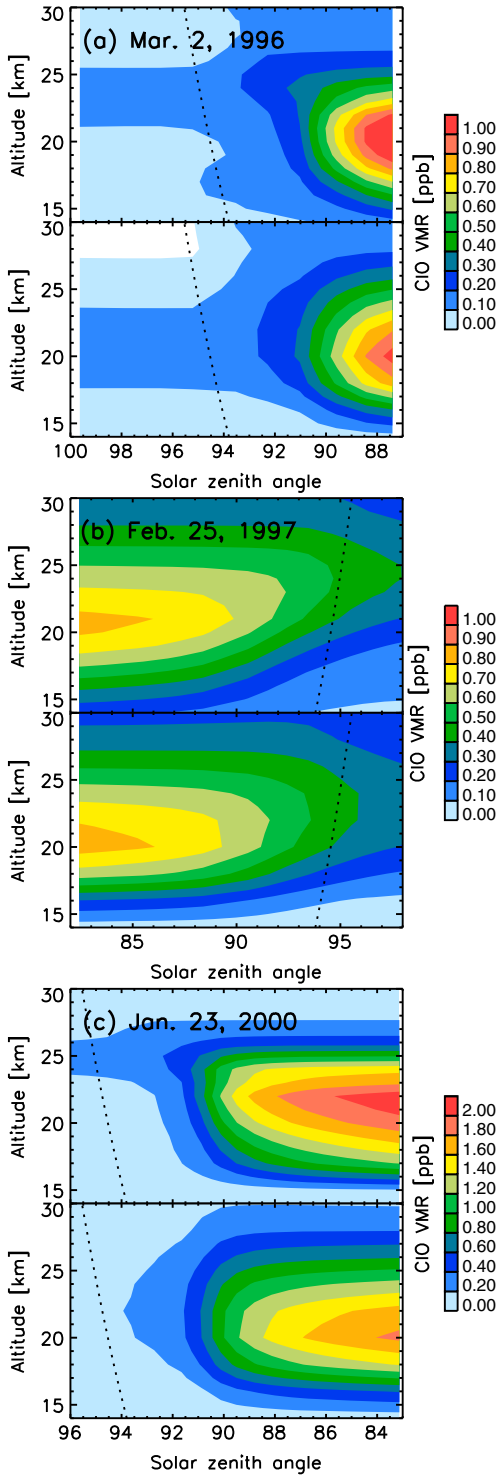

Figure 8. Color-contoured ClO volume mixing ratio profiles modeled by the MISU-1D model for the flights shown in Figure 3. (top) Panels in each plot show the ClO mixing ratios of the high-resolution profiles, while (bottom) panels in each plot show the ClO profiles after being convolved with the ASUR averaging kernels. The dotted line indicates the astronomical terminator.

Contour plots of the simulated ClO profiles are presented in Figure 8 using photolysis cross sections recommended in *Sander et al.* [2003] and an equilibrium constant recommended in *Sander et al.* [2009]. The top panels of the individual plots in Figure 8 give the results on the original altitude grid used in the model. For the January 2000 flight, profile (b) from Figure 6 was used for subsequent modeling. For the other flights, high-resolution profiles were constructed analogously. To account for the limited vertical resolution of the measurements, the modeled ClO profiles were smoothed using the a priori information and averaging kernel functions shown in Figure 2. The bottom panels for each flight in Figure 8 show the modeled ClO profiles after this smoothing has been applied.

The ClO distributions in Figure 8 qualitatively agree very well with the observed diurnal variation of ClO (Figure 3). For the sunrise flight in 1996, ClO starts building up slowly after astronomical sunrise. This is well represented by the model in Figure 8. For the sunrise flight in 2000, the measurements in Figure 3 might suggest a slight delay in the buildup of ClO past the terminator. *Wetzel et al.* [2012] presented a case where the onset of ClO at sunrise was significantly delayed, which was attributed to polar stratospheric clouds (PSCs) influencing the levels of UV radiation available for dimer photolysis. The buildup of ClO for the 2000 flight seems to occur more slowly than in *Wetzel et al.* [2012], and the slow increase is well represented by the model calculations, which do not take scattering or absorption due to PSCs into account in the radiative transfer. The overall good agreement between the measurements and the model calculations at sunrise suggests that PSCs were unlikely to have had a major influence on the radiative transfer and the onset of ClO-dimer photolysis.

As the behavior of ClO at sunrise might be influenced by air parcel history due to the buildup of Cl_2 in darkness [*Wilmouth et al.*, 2006], back trajectories from measurements of both the 2000 and the 1996 flights were calculated using a kinematic back trajectory model [*Schoeberl and Sparling*, 1995] with National Centers for Environmental Prediction (NCEP)/National Center for Atmospheric Research reanalysis winds [*Randel*, 1987]. Both the sunlight history for several days along the trajectories as well as the temperature history along the trajectories in comparison to the formation temperature of nitric acid trihydrate (T_{NAT}) were studied. Figure 9 shows examples for the high-Sun measurements of both flights. T_{NAT} was calculated

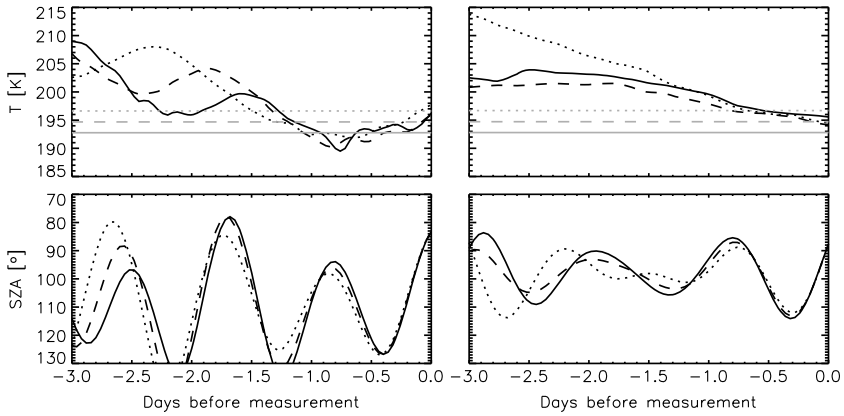

Figure 9. (top) Temperature and (bottom) SZA along back trajectories started at pressure levels corresponding to altitudes of 18 km (black, dotted), 20 km (black, dashed), and 22 km (black, solid) for the high-Sun measurements of (left) the January 2000 flight and (right) the March 1996 flight. The gray lines in Figure 9 (top) show the formation temperatures of nitric acid trihydrate for the pressure levels corresponding to 18 km (dotted), 20 km (dashed), and 22 km (solid) altitude.

using the formulation by *Hanson and Mauersberger* [1988] with input VMRs of 8 ppb HNO_3 and 5 ppm H_2O. These values are realistic for the January 2000 [*Kleinböhl et al.*, 2002] and for the early-March 1996 [*Santee et al.*, 1996] Arctic lower stratosphere. For the January 2000 flight, the trajectories indicate that for lower stratospheric altitudes between 18 and 22 km, the air masses had experienced SZAs below 85° and temperatures above T_{NAT} between 1.5 and 2 days before the measurement and at 18 km also between 2.5 and 3 days before the measurement. For altitudes around 22 km, the temperature only dropped below T_{NAT} for a few hours within the day before the measurement, suggesting that little chlorine activation could have taken place that could lead to the buildup of Cl_2. Air masses at altitudes around 20 km and below experienced temperatures below T_{NAT} for several hours and SZAs only at or above 96° during the day before the measurement. According to *Wilmouth et al.* [2006], this can lead to the buildup of Cl_2 to a level that can influence the chlorine budget. We note that the potential presence of Cl_2 does not influence the results presented in section 3.1 because the high-Sun ClO profile of the January 2000 flight had been experiencing SZAs below 90° for about 2 h prior to the measurement, which suggests that any Cl_2 that might have been present should have mostly photolyzed by the time of measurement [*Wilmouth et al.*, 2006]. For the March 1996 flight, the trajectories show that the air masses at lower stratospheric altitudes had all been exposed to sunlight below 89° SZA within the day before the measurement. Temperatures tended to be above T_{NAT} at altitudes of 20 km and higher; only around 18 km the air mass experienced temperatures below T_{NAT} for a few hours. This trajectory analysis indicates that conditions were not conducive to the buildup of Cl_2 in amounts sufficient to significantly influence the chlorine budget for air parcels sampled by ASUR.

The sensitivity of the diurnal variation of ClO at 20 km to various measurements of the ClO-dimer cross section is presented in Figure 10. The results shown in the figure cover the range from fast photolysis frequencies [e.g., *Papanastasiou et al.*, 2009] to comparatively slow photolysis frequencies [*von Hobe et al.*, 2009]. The simulations have been constrained to match observed ClO during high-Sun conditions by allowing ClO_x to vary; different values of ClO_x are associated with various estimates of the Cl_2O_2 cross section. The part of the diurnal behavior of ClO that is most sensitive to the photolysis frequency is the curvature of the rate of change in ClO mixing ratio for values of SZA between 80° and 90°. The simulations were performed without considering a potential contribution of Cl_2 photolysis to the ClO production, which could influence the rate of ClO increase at sunrise. We note that the results in Figure 10 are mixing ratios after convolution with the ASUR averaging kernels. They consider ClO contributions from above 20 km, which should be largely unaffected by Cl_2 buildup, as well as from below 20 km, which might have been affected, such that the overall effect of Cl_2 buildup should be less severe than if the VMR at an individual altitude level were considered. Assuming that the influence of Cl_2 photolysis on the results in Figure 10 is small, photolysis frequencies based on cross sections from *Papanastasiou et al.* [2009] and *Sander et al.* [2003] reproduce this curvature reasonably well in the January 2000 sunrise flight. Cross sections leading to slower rates tend to result in a flatter curvature in this SZA range, which would corroborate the results presented in section 3.1.

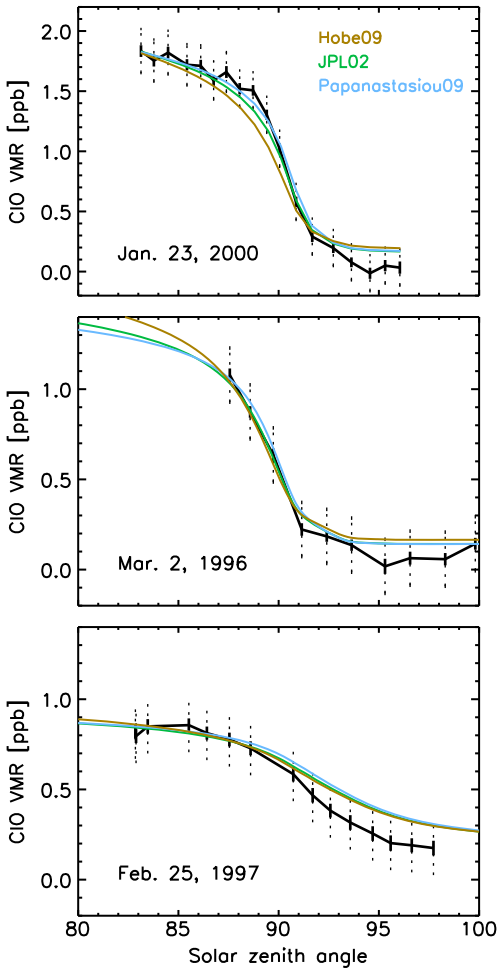

Figure 10. Modeled ClO mixing ratios for the three flights at 20 km altitude, convolved with the ASUR averaging kernels. Calculations were done for different photolysis cross sections by *Papanastasiou et al.* [2009] (blue), *Sander et al.* [2003] (green), and *von Hobe et al.* [2009] (brown). All calculations use the equilibrium constant by *Sander et al.* [2009]. The black lines show the ClO measured by ASUR, with the solid error bars giving the precision and the dotted error bars giving the accuracy.

The observations in March 1996 do not reach to low enough SZAs to allow the plausibility of various absorption cross sections to be assessed. We investigated the influence of the wind speed on the change of ClO across the terminator based on air parcel trajectories. For sunrise conditions, this influence is small (< 5% between 85° and 90° SZA). For the sunset flight in February 1997, the calculations with different photolysis cross sections lead to very similar ClO VMRs. For all flights, the measured ClO tends to be lower than the calculated ClO at high SZAs, which will be discussed in the following sections.

3.3. Study of the Equilibrium Constant

During nighttime, the loss of ClO-dimer in the polar lower stratosphere occurs exclusively by thermal decomposition. The kinetics of the partitioning of ClO and ClO-dimer during nighttime have been addressed in a number of studies [e.g., *Avallone and Toohey*, 2001; *Cox and Hayman*, 1988; *Nickolaisen et al.*, 1994; *Plenge et al.*, 2005; *Stimpfle et al.*, 2004; *von Hobe et al.*, 2005] and were summarized by *von Hobe et al.* [2007] and *SPARC* [2009].

Values of K_{eq} from *Avallone and Toohey* [2001], *von Hobe et al.* [2005], and JPL recommendations were used and compared with observations to test our understanding of nighttime ClO_x photochemistry. The rate constants are summarized in Table 3. The results are presented in Figure 11 for the 20 km altitude level. Photolysis frequencies based on cross sections recommended by *Sander et al.* [2003] were used for these calculations. The sensitivity of ClO to various values of K_{eq} is most apparent when the ClO mixing ratio levels off at higher SZAs. All equilibrium constants used in these simulations tend to overestimate the measured nighttime abundance of ClO. Among different parameterizations, the JPL recommendation of 2000 [*DeMore et al.*, 2000] yields very low ClO values at high solar zenith angles, comparable to those from the recommendation of 2006 [*Sander et al.*, 2006] and slightly lower than those from the recommendation of 2009 [*Sander et al.*, 2009] (not shown). Slightly higher nighttime ClO mixing ratios result from the equilibrium constant suggested by *Avallone and Toohey* [2001], while *von Hobe et al.* [2005] give by far the highest calculated ClO.

Table 3. Parameters Used to Calculate the Different Equilibrium Constants According to the Equation $K_{eq} = A \cdot e^{B/T}$ With T Being the Temperature

Data Set No.	A $\left(\frac{cm^3}{molecule}\right)$	B (K)	Reference
1	$1.27 \cdot 10^{-27}$	8744	*DeMore et al.* [2000]
2	$9.3 \cdot 10^{-28}$	8835	*Sander et al.* [2006]
3	$1.72 \cdot 10^{-27}$	8649	*Sander et al.* [2009]
4[a]	$1.99 \cdot 10^{-30}$	8854	*Avallone and Toohey* [2001]
5	$3.61 \cdot 10^{-27}$	8167	*von Hobe et al.* [2005]

[a]For the parameters by *Avallone and Toohey* [2001], the equation is $K_{eq} = A \cdot T \cdot e^{B/T}$.

As calculated ClO depends on both the temperature and the amount of available ClO_x, which in turn depends on the ClO-dimer cross section, we perform sensitivity studies to evaluate these influences. We assume an error in ClO_x based on the accuracy of the ASUR ClO at high

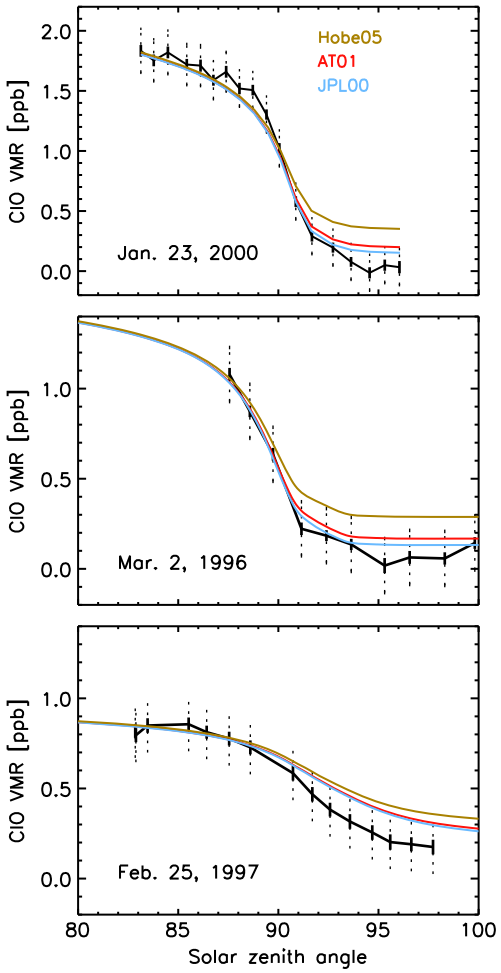

Figure 11. Modeled ClO mixing ratios for the three flights at 20 km altitude, convolved with the ASUR averaging kernels. Calculations were done for different equilibrium constants by *DeMore et al.* [2000] (blue), *Avallone and Toohey* [2001] (red), and *von Hobe et al.* [2005] (brown). All calculations use photolysis frequencies from *Sander et al.* [2003]. The black lines show the ClO measured by ASUR, with the solid error bars giving the precision and the dotted error bars giving the accuracy.

Sun and a 2 K error in temperature. Figure S2 in the supporting information compares temperature profiles measured by the ER-2 and ozone sondes close to the locations of the ASUR measurements to the NCEP meteorological analyses used in the retrieval and modeling, and shows that this is a reasonable confidence interval for temperature. Tests to investigate the influence of the shape of the input ClO_x profile suggest that the influence of the profile shape is smaller than the influence of the choice of the photolysis cross sections used to estimate ClO_x. Figure 12 summarizes these sensitivity studies. We focus on the sunrise measurements obtained at SZA$\geq$ 96° because the influence of photolysis is small for these conditions. Values of ClO calculated with different JPL recommendations for K_{eq} are within the accuracies of the ASUR ClO measurements for all input ClO_x profiles. ClO calculated using K_{eq} from *Avallone and Toohey* [2001] is within the accuracies of the measurements in March 1996. For the January 2000 measurement, the *Avallone and Toohey* [2001] calculation results in ClO that is slightly higher than observed ClO. However, considering the uncertainties in input ClO_x and temperature, there is still reasonable agreement. For ClO calculated with K_{eq} from *von Hobe et al.* [2005], agreement is only achieved for the March 1996 measurement at the highest SZA using the ClO-dimer cross sections that yield lowest values of ClO_x. For the other measurements from March 1996, error bars for modeled nighttime ClO only overlap measured ClO error bars at the low edge of the considered temperature range, while for the January 2000 measurement, no overlap is achieved within the respective uncertainties. If some Cl_2 buildup had occurred in the conditions of January 2000, some of the ClO observed in the high-Sun measurement could have originated from the photolysis of Cl_2, leading to an overestimate of ClO_x and hence ClO in darkness. The fact that the differences between measured and calculated ClO in darkness are slightly larger in the 2000 flight than in the 1996 flight might point to an influence of this effect. However, the behavior observed in January 2000 is still similar to the March 1996 measurements, making the value of K_{eq} by *von Hobe et al.* [2005] less plausible than the other equilibrium constants, in agreement with previous studies [*von Hobe et al.*, 2007; *Santee et al.*, 2010].

3.4. Study of the Influence of the ClO + BrO Reaction

In addition to reactions related to ClO-dimer, the behavior of ClO in twilight conditions is influenced by the reaction between ClO and BrO, given in equations (9)–(11). Sensitivity studies show that during sunrise, uncertainties in the ClO + BrO product yields modify ClO only in a narrow range of SZAs around 92°. During sunset, in contrast, ClO mixing ratios are significantly altered starting around 91° SZA and lasting well into night (i.e., beyond 100° SZA).

We investigate the influence of ClO + BrO reaction product yields using the sunset flight from 25 February 1997. ClO VMRs measured by ASUR tended to be lower than calculated by the MISU-1D model beyond ~ 91°

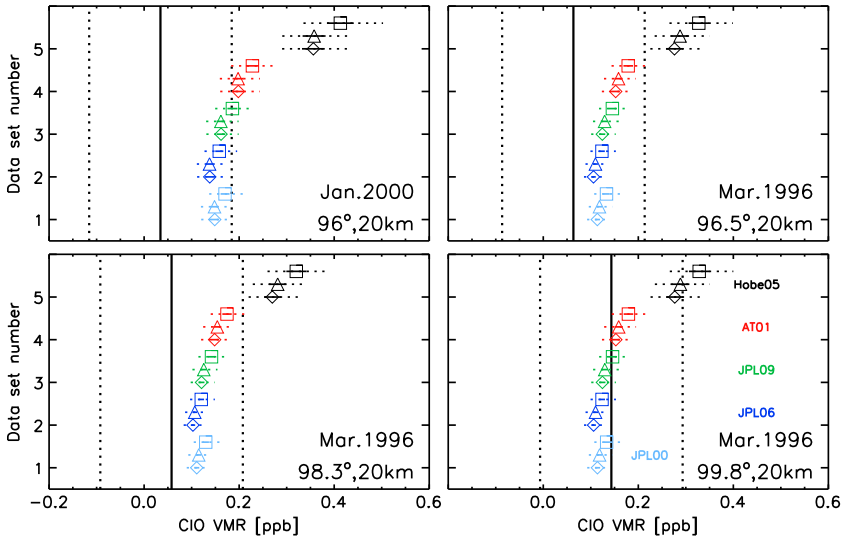

Figure 12. Comparison of nighttime ClO calculated from ClO_x derived from ClO at high Sun (colored symbols) with ClO measured by ASUR at SZA≥ 96° (vertical solid black lines with dotted lines giving the accuracy) for 20 km altitude. ClO was calculated using different equilibrium constants according to the data set number (1: JPL00 [*DeMore et al.*, 2000], 2: JPL06 [*Sander et al.*, 2006], 3: JPL09 [*Sander et al.*, 2009], 4: *Avallone and Toohey* [2001], and 5: *von Hobe et al.* [2005]) using input ClO_x profiles based on cross sections by *Papanastasiou et al.* [2009] (diamonds), *Sander et al.* [2003] (triangles), and *von Hobe et al.* [2009] (squares), and convolved with the ASUR averaging kernels. Solid error bars give the uncertainty based on the accuracy of the ASUR ClO at high Sun, dashed error bars additionally include a temperature error of 2 K.

SZA (Figure 10). We use the calculation based on photolysis cross sections recommended by *Sander et al.* [2003] and the equilibrium constant by *Sander et al.* [2009] as the baseline case (green line in Figure 10). It yields OClO mixing ratios of about 80 ppt at nighttime. We perturb the rate constants for the ClO + BrO reaction by the uncertainties given in *Sander et al.* [2009]. The uncertainty of reactions (9)–(11) is estimated to be a factor of 1.2 at 298 K. The uncertainty in the overall rate of reactions (9)–(11) rises to 1.44 at 190 K, a typical temperature around 20 km altitude along the flight path. Calculations were performed in which the reaction rate for each individual branch of the ClO + BrO reaction was varied by a factor 1.44. The rate of formation of ClOO (reaction (10)) has an insignificant impact on calculated ClO because of the rapid thermal decomposition of ClOO. Hence, Figure 13 shows model results only for variations in the rate of formation of OClO (reaction (9)) and BrCl (reaction (11)).

Increasing the rate of formation of OClO by the JPL uncertainty leads to a decrease in calculated ClO by about 7% for SZAs between 95° and 100°. This model result is found because the other product of reaction (9) is Br. As the rate of this channel rises, higher abundances of BrO persist into twilight. Higher BrO in twilight forces a greater fraction of ClO to be sequestered as OClO, which is thermally stable, rather than Cl_2O_2, which reaches a thermal equilibrium. In contrast, a decrease in the rate of reaction (11) by the JPL uncertainty leads to a decline in ClO during twilight, because the sequestration of BrO into its nighttime reservoir BrCl is suppressed. This again allows for a larger fraction of daytime ClO to be sequestered at night into the thermally stable OClO, and leads to higher BrO amounts persisting into twilight. The ClO deviation due to reaction (11) sets in slightly later than the change due to (9) but reaches a higher magnitude at larger SZAs.

Figure 13 also shows a model simulation in which the rate of reaction (9) has been perturbed upward and the rate of reaction (11) has been perturbed downward by their respective uncertainties. The calculation yields a ClO mixing ratio that is 11% lower at 95° SZA, and 24% lower at 100° SZA compared to the standard case. While the ASUR measurements within their precisions still show ClO VMRs lower than the calculations, the perturbation of both branches brings the calculated ClO significantly closer to the measurements, suggesting that the ClO + BrO reaction may bind more ClO as OClO at sunset than is currently assumed.

Also included in Figure 13 is a sensitivity study where a perturbation of ±2 K is applied to the temperature profile assumed in the model run. Figure S2 in the supporting information demonstrates that this estimate for the uncertainty in temperature is realistic. The discrepancy between measured and modeled ClO is

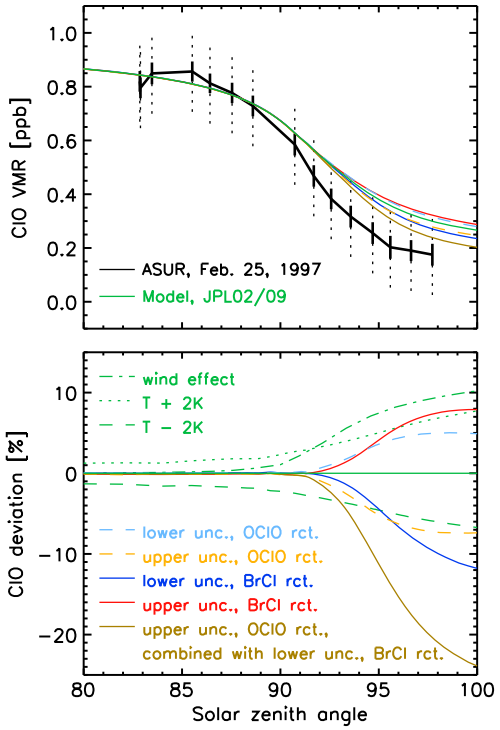

Figure 13. (top) Modeled ClO mixing ratios for the sunset flight on 25 February 1997 at 20 km altitude, convolved with the ASUR averaging kernels. Calculations were done with photolysis cross sections in *Sander et al.* [2003] and ClO-dimer equilibrium and ClO + BrO rate constants in *Sander et al.* [2009] (green). The ClO + BrO rate constant was varied by its uncertainty downward in the branch forming OClO (light blue), upward in the branch forming OClO (yellow), downward in the branch forming BrCl (blue), and upward in the branch forming BrCl (red). Also shown is an upward perturbation in the OClO branch combined with a downward perturbation in the BrCl branch (brown). The black line shows the ClO measured by ASUR, with the solid error bars giving the precision and the dotted error bars giving the accuracy. (bottom) Percentage difference in ClO VMR between the standard case and the different perturbations to the ClO + BrO reaction. The color coding is identical to the top plot. The green lines show the effect on ClO of a ±2 K T uncertainty (dotted and dashed lines) and the effect on ClO of wind moving an air parcel along a predominantly west to east trajectory, which is simulated by assuming a 20 h day in the model (dash-dotted line).

considerably larger than the uncertainty attributed to a ±2 K error in temperature. Nonetheless, the sensitivity to temperature is important as it is comparable in magnitude to some of the suggested perturbations to the governing rate constants. Air parcel trajectory simulations conducted for the February 1997 flight suggest that the wind was essentially in the west to east direction, compressing the length of the day by about 15% compared to a stationary observer. This effect was simulated by assuming a 20 h day in the model instead of a 24 h day. The result is shown by the green dash-dotted line in Figure 13. The calculated abundance of ClO is ~10% higher after sunset compared to the stationary simulation. This moves the model result further away from the measured ClO values, underlining the relevance of the discrepancy between the measurement and the model result.

A concern with the current analysis could be the introduction of nitrogen oxides (NO_x) at the sunset transition, which could influence the decrease of ClO. *Pierce et al.* [1997] reported observations by the Halogen Occultation Experiment that show NO_x levels around 1 ppb in the Arctic vortex in late-March 1997. The trend of about 1 ppb/month they derived during this season suggests that NO_x levels should still have been very low during the time of the ASUR measurement. If low levels of NO_x were present, NO_2 would quickly react with ClO, forming $ClNO_3$, the diurnal variation of which is very small in the lower stratosphere. The main source of NO_x is the photolysis of HNO_3, which is very slow, such that any NO_x would be introduced slowly and is hence unlikely to influence the decrease of ClO. Short-lived reservoirs of NO_x, e.g., HNO_4, have the potential to influence the decrease of ClO as they photolyze more rapidly. We considered HNO_4 measured by MkIV in March 2000, which is the closest measurement available in terms of region and season. Levels of HNO_4 were found to be in the order of 30 ppt in the lower stratosphere, suggesting that it did not have a significant influence as a source of NO_x.

Our suggestion that the yield of BrCl from ClO + BrO lies at the lower limit of the kinetics uncertainty is at odds with findings of *Canty et al.* [2005] and *Butz et al.* [2007]. *Canty et al.* [2005] showed an analysis of nighttime OClO that could only be reconciled with a simulation that placed the BrCl yield at its upper limit, whereas *Butz et al.* [2007] showed twilight observations of OClO that are simulated well by a model using the recommended baseline yield for BrCl. In situ measurements have shown significant amounts of BrO in the activated vortex at twilight [*Avallone and Toohey*, 2001] but no BrO in darkness [*Toohey et al.*, 1990]. *Avallone and Toohey* [2001] suggested the weakly bound adduct BrOOCl as a temporary reservoir of BrO, which has been studied theoretically but not in the laboratory. The dissociation of BrOOCl could lead to an increased availability of BrO in twilight, which in turn would allow a larger fraction of ClO to be sequestered as OClO, hence lowering ClO in twilight. The details of this process, and whether it would allow a reconciliation of

the above findings, would be determined by the thermal and photolytical stability of BrOOCl. This points to a need for more work in this area, in particular laboratory measurements of BrOOCl and simultaneous measurements of ClO, BrO, and OClO in the atmosphere during the day to night transition.

4. Conclusions

Significant differences exist between various laboratory measurements of the absorption cross sections of ClO-dimer, and the rate constant controlling the thermal equilibrium between ClO-dimer and ClO. Uncertainties in the ClO-dimer cross section have a strong effect on the calculations of stratospheric ozone loss in the winter polar regions [e.g., *von Hobe et al.*, 2007; *Kawa et al.*, 2009; *SPARC*, 2009]. We constrain the plausibility of these parameters by measuring ClO across the terminator in the activated Arctic polar vortex.

ClO-dimer absorption cross sections leading to fast photolysis frequencies such as *Burkholder et al.* [1990] or *Papanastasiou et al.* [2009] give ClO_x mixing ratios that overlap with our estimated range of available Cl_y. ClO_x values based on the recent cross-section measurements by *Young et al.* [2014] are higher than the ones calculated based on *Papanastasiou et al.* [2009] but are still within the Cl_y range for some of the conditions considered. Photolysis frequencies based on cross sections by *von Hobe et al.* [2009] and *Huder and DeMore* [1995] lead to ClO_x values that are higher than the available Cl_y. ClO_x values calculated with cross sections by *Pope et al.* [2007] have to be considered unrealistically large given our present understanding of chlorine chemistry, as suggested by previous studies [e.g., *Chen et al.*, 2009; *Papanastasiou et al.*, 2009; *Kremser et al.*, 2011; *Suminska-Ebersoldt et al.*, 2012].

Scaling the ClO-dimer absorption cross sections considered here to the absolute measurements at 248 nm reported by *Lien et al.* [2009] leads to faster photolysis of Cl_2O_2 and a reduction in the amount of ClO_x. Using the absolute cross section measured by *Lien et al.* [2009] at 248 nm to scale the cross-section spectra reduces the ClO_x values calculated with the JPL 2002 recommendation such that they overlap with the available Cl_y. Recent work by *Suminska-Ebersoldt et al.* [2012] suggests photolysis frequencies between the ones resulting from cross sections by *Papanastasiou et al.* [2009] and *von Hobe et al.* [2009] scaled to Lien09. Our results show that the fast photolysis frequencies in the range suggested by *Suminska-Ebersoldt et al.* [2012] are plausible; however, cross sections by *von Hobe et al.* [2009], *Huder and DeMore* [1995], and *Pope et al.* [2007] still produce ClO_x values that are higher than the available Cl_y, even when these cross sections are scaled to Lien09. The latest version of the kinetics evaluation by the Jet Propulsion Laboratory [*Sander et al.*, 2011] now recommends the cross sections by *Papanastasiou et al.* [2009] for use in kinetic studies. Our results support this recommendation.

Calculations with equilibrium constants published in the JPL kinetics evaluation of the last few years all give good agreement with observed nighttime mixing ratios of ClO. The equilibrium constant estimated by *von Hobe et al.* [2005] yields nighttime ClO values that are higher than observed. This is in agreement with the analysis of nighttime ClO at cold temperatures reported by *Berthet et al.* [2005], which also concluded that the introduction of K_{eq} given by *von Hobe et al.* [2005] at temperatures below ~200 K leads to an overestimation of ClO in their model. Results based on nighttime ClO data from the Microwave Limb Sounder on EOS-Aura [*Santee et al.*, 2010] suggest an equilibrium constant in agreement with *Avallone and Toohey* [2001] and close to the ones recommended in the JPL kinetics evaluations of the recent years [*Sander et al.*, 2006, 2009]. Our analysis largely supports this conclusion.

To study the influence of the reaction of ClO + BrO on the ClO VMR at sunset, we performed calculations that varied the rates of each branch of this reaction by the uncertainty given in *Sander et al.* [2009]. We find that the agreement with measurements is improved by increasing the rate of the branch-forming OClO and by decreasing the rate of the branch-forming BrCl, suggesting that the ClO + BrO reaction may bind more ClO as OClO at sunset than currently assumed.

Acknowledgments

We are grateful to H. Bremer and M. Sinnhuber for their contributions to data acquisition and retrieval of ASUR data. We would like to acknowledge V. Eyring for performing initial analyses of the flights from 1996 and 1997, and we would like to thank Y. Tijani for re-integrating the ASUR measurements of the 1996/1997 flights. We are grateful to K. Künzi for providing the opportunity to perform measurements with ASUR on board of research aircraft. We also thank G. Näveke, N. Whyborn, H. Golstein, and H. Schaeffer for their excellent technical support prior to and during the ASUR aircraft campaigns. We are thankful to R. M. Stimpfle, D. M. Wilmouth, and J. G. Anderson for providing their ClO and $ClNO_3$ measurements from the ER-2 via the NASA ESPO archive. We thank the aircraft crew of the DLR Falcon for their support during the 1996/1997 campaigns. We are grateful for the opportunity to participate on board the NASA DC-8 during SOLVE and thank the aircraft crew for their support. We want to express our gratitude to J.-F. L. Blavier, D. Petterson, and J. Landeros for their contributions to the balloon flight from Esrange. We thank NASA CSBF for performing the balloon launch and for their support during the campaign. We acknowledge GMAO and NCEP for providing meteorological analyses. T. Canty and R. Salawitch appreciate support from the Atmospheric Composition, Modeling, and Analysis Program of the National Aeronautics and Space Administration. Work at the Jet Propulsion Laboratory, California Institute of Technology, is performed under a contract with the National Aeronautics and Space Administration.

References

Avallone, L. M., and D. W. Toohey (2001), Tests of halogen photochemistry using in situ measurements of ClO and BrO in the lower polar stratosphere, *J. Geophys. Res.*, *106*, 10,411–10,421.

Berthet, G., P. Ricaud, F. Lefèvre, E. Le Flochmoën, J. Urban, B. Barret, N. Lautié, E. Dupuy, J. De La Noë, and D. Murtagh (2005), Nighttime chlorine monoxide observations by the Odin satellite and implications for the ClO/Cl_2O_2 equilibrium, *Geophys. Res. Lett.*, *32*, L11812, doi:10.1029/2005GL022649.

Bloss, W. J., S. L. Nickolaisen, R. J. Salawitch, R. R. Friedl, and S. P. Sander (2001), Kinetics of the ClO self-reaction and 210 nm absorption cross-section of the ClO dimer, *J. Phys. Chem.*, *105*, 11,226–11,239.

Bremer, H., M. von König, A. Kleinböhl, H. Küllmann, K. Künzi, K. Bramstedt, J. P. Burrows, K.-U. Eichmann, M. Weber, and A. P. H. Goede (2002), Ozone depletion observed by ASUR during the Arctic winter 1999/2000, *J. Geophys. Res.*, *107*(D20), 8277, doi:10.1029/2001JD000546.

Brune, W. H., D. W. Toohey, J. G. Anderson, and K. R. Chan (1990), In situ observations of ClO in the Arctic stratosphere: ER-2 aircraft results from 59°N to 80°N latitude, *Geophys. Res. Lett.*, *17*, 505–508.

Burkholder, J. B., J. J. Orlando, and C. J. Howard (1990), Ultraviolet absorption cross-sections of Cl_2O_2 between 210 and 410 nm, *J. Phys. Chem.*, *94*, 687–695.

Butz, A., H. Bösch, C. Camy-Peyret, M. Dorf, A. Engel, S. Payan, and K. Pfeilsticker (2007), Observational constraints on the kinetics of the ClO-BrO and ClO-ClO ozone loss cycles in the Arctic winter stratosphere, *Geophys. Res. Lett.*, *34*, L05801, doi:10.1029/2006GL028718.

Canty, T., et al. (2005), Nighttime OClO in the winter arctic vortex, *J. Geophys. Res.*, *110*, D01301, doi:10.1029/2004JD005035.

Chen, H.-Y., C.-Y. Lien, W.-Y. Lin, Y. T. Lee, and J. J. Lin (2009), UV absorption cross sections of ClOOCl are consistent with ozone degradation models, *Science*, *324*, 781–784.

Chipperfield, M. P., W. Feng, and M. Rex (2005), Arctic ozone loss and climate sensitivity: Updated three-dimensional model study, *Geophys. Res. Lett*, *32*, L11813, doi:10.1029/2005GL022674.

Coffey, M. T., W. G. Mankin, J. W. Hannigan, and G. C. Toon (2002), Airborne spectroscopic observations of chlorine activation and denitrification of the 1999/2000 winter Arctic stratosphere during SOLVE, *J. Geophys. Res.*, *107*(D5), 8303, doi:10.1029/2001JD001085, [printed 108(D5), 2003].

Cox, R. A., and G. Hayman (1988), The stability and photochemistry of the dimers of the ClO radical and implications for Antarctic ozone depletion, *Nature*, *332*, 796–800.

DeMore, W. B., et al. (2000), Chemical kinetics and photochemical data for use in stratospheric modeling, *Tech. Rep. 00-3*, Jet Propul. Lab., Pasadena, Calif.

Dorf, M., J. H. Butler, A. Butz, C. Camy-Peyret, M. P. Chipperfield, L. Kritten, S. A. Montzka, B. Simmes, F. Weidner, and K. Pfeilsticker (2006), Long-term observations of stratospheric bromine reveal slow down in growth, *Geophys. Res. Lett.*, *33*, L24803, doi:10.1029/2006GL027714.

Drdla, K., and R. Müller (2012), Temperature thresholds for chlorine activation and ozone loss in the polar stratosphere, *Ann. Geophys.*, *30*, 1055–1073.

Eyring, V. (1999), Model studies on the Arctic stratospheric chemistry compared to measurements, *Reports on Polar Research*, Alfred-Wegener-Institute for Polar and Marine Research, Bremerhaven, Germany.

Friedl, R. R., and S. P. Sander (1989), Kinetics and product studies of the reaction ClO + BrO using discharge-flow mass spectrometry, *J. Phys. Chem.*, *93*, 4756–4764.

Frieler, K., M. Rex, R. J. Salawitch, T. Canty, M. Streibel, R. M. Stimpfle, K. Pfeilsticker, M. Dorf, D. K. Weisenstein, and S. Godin-Beekmann (2006), Toward a better quantitative understanding of polar stratospheric ozone loss, *Geophys. Res. Lett*, *33*, L10812, doi:10.1029/2005GL025466.

Greenblatt, J. B., et al. (2002), Tracer-based determination of vortex descent in the 1999/2000 Arctic winter, *J. Geophys. Res.*, *107*(D20), 8279, doi:10.1029/2001JD000937.

Hanson, D., and K. Mauersberger (1988), Laboratory studies of the nitric acid trihydrate: Implications for the south polar stratosphere, *Geophys. Res. Lett.*, *15*, 855–858.

Huder, K. J., and W. B. DeMore (1995), Absorption cross sections of the ClO dimer, *J. Phys. Chem.*, *99*, 3905–3908.

Jin, B., I.-C. Chen, W.-T. Huang, C.-Y. Lien, N. Guchhait, and J. J. Lin (2010), Photodissociation cross section of ClOOCl at 330 nm, *J. Phys. Chem.*, *114*, 4791–4797.

Jonsson, A. (2006), Modelling the middle atmosphere and its sensitivity to climate change, PhD thesis, Stockholm Univ., Sweden.

Kawa, S. R., D. W. Fahey, L. E. Heidt, W. H. Pollock, S. Solomon, D. E. Anderson, M. Loewenstein, M. H. Proffitt, J. J. Margitan, and K. R. Chan (1992), Photochemical partitioning of the reactive nitrogen and chlorine reservoirs in the high-latitude stratosphere, *J. Geophys. Res.*, *97*, 7905–7923.

Kawa, S. R., R. S. Stolarski, P. A. Newman, A. R. Douglass, M. Rex, D. J. Hofmann, M. L. Santee, and K. Frieler (2009), Sensitivity of polar stratospheric ozone loss to uncertainties in chemical reaction kinetics, *Atmos. Chem. Phys.*, *9*, 8651–8660.

Khosravi, M., et al. (2013), Diurnal variation of stratospheric HOCl, ClO and HO_2 at the equator: Comparison of 1-D model calculations with measurements of satellite instruments, *Atmos. Chem. Phys.*, *13*, 7587–7606.

Kivi, R., E. Kyrö, T. Turunen, N. R. P. Harris, P. von der Gathen, M. Rex, S. B. Andersen, and I. Wohltmann (2007), Ozonesonde observations in the Arctic during 1989–2003: Ozone variability and trends in the lower stratosphere and free troposphere, *J. Geophys. Res.*, *112*, D08306, doi:10.1029/2006JD007271.

Kleinböhl, A., et al. (2002), Vortexwide denitrification of the Arctic polar stratosphere in winter 1999/2000 determined by remote observations, *J. Geophys. Res.*, *107*(D5), 8305, doi:10.1029/2001JD001042, [printed 108(D5), 2003].

Koppers, G. A. A., and D. P. Murtagh (1996), Model studies of the influence of O_2 photodissociation parametrizations in the Schumann-Runge bands on ozone related photolysis on the upper atmosphere, *Ann. Geophys.*, *14*, 68–79.

Kremser, S., et al. (2011), Retrievals of chlorine chemistry kinetic parameters from Antarctic ClO microwave radiometer measurements, *Atmos. Chem. Phys.*, *11*, 5183–5193.

Lien, C.-Y., W.-Y. Lin, H.-Y. Chen, W.-T. Huang, B. Jin, I.-C. Chen, and J. J. Lin (2009), Photodissociation cross sections of ClOOCl at 248.4 and 266 nm, *J. Chem. Phys.*, *131*, 174,301, doi:10.1063/1.3257682.

Madronich, S. (1993), The atmosphere and UV-B radiation at ground level, in *Environmental UV Photobiology*, edited by A. R. Young et al., pp. 345–377, Plenum Press, New York.

McElroy, M. B., R. J. Salawitch, S. C. Wofsy, and J. A. Logan (1986), Reductions of Antarctic ozone due to synergistic interactions of chlorine and bromine, *Nature*, *321*, 759–762.

McGrath, M. P, K. C. Clemitshaw, F. S. Rowland, and W. J. Hehre (1988), Thermochemical stabilities and vibrational spectra of isomers of the chlorine oxide dimer, *Geophys. Res. Lett.*, *15*, 883–886.

Meier, R. R., D. E. Anderson Jr., and M. Nicolet (1982), Radiation field in the troposphere and stratosphere from 240–1000 nm - I. General analysis, *Planet. Space Sci.*, *30*, 923–933.

Molina, L. T., and M. J. Molina (1987), Production of Cl_2O_2 from the self-reaction of the ClO radical, *J. Phys. Chem.*, *91*, 433–436.

Montzka, S. A., R. C. Myers, J. H. Butler, J. W. Elkins, L. T. Lock, A. D. Clarke, and A. H. Goldstein (1999), Present and future trends in the atmospheric burden of ozone-depleting halogens, *Nature*, *398*, 690–694.

Nickolaisen, S. L., R. R. Friedl, and S. P. Sander (1994), Kinetics and mechanism of the ClO+ClO reaction/pressure and temperature dependecies of the bimolecular and termolecular channels and thermal decomposition of chlorine peroxide, *J. Phys. Chem.*, *98*, 155–169.

Nicolet, M., and R. Kennes (1986), Aeronomic problems of the molecular oxygen photodissociation I. The O_2 Herzberg continuum, *Planet. Space Sci.*, *34*, 1043–1059.
O'Doherty, S., et al. (2004), Rapid growth of hydrofluorocarbon 134a, and hydrochlorofluorocarbons 141b, 142b and 22 from Advanced Global Atmospheric Gases Experiment AGAGE observations at Cape Grim, Tasmania, and Mace Head, Ireland, *J. Geophys. Res.*, *109*, D06310, doi:10.1029/2003JD004277.
Papanastasiou, D. K., V. C. Papadimitriou, D. W. Fahey, and J. B. Burkholder (2009), UV absorption spectrum of the ClO dimer (Cl_2O_2) between 200 and 420 nm, *J. Phys. Chem.*, *113*, 13,711–13,726.
Pierce, R. B., T. D. Fairlie, E. E. Remsberg, Russel III, J. M., and W. L. Grose (1997), HALOE observations of the Arctic vortex during the 1997 spring: Horizontal structure in the lower stratosphere, *Geophys. Res. Lett.*, *24*, 2701–2704.
Pierson, J. M., K. A. McKinney, D. W. Toohey, U. Schmidt, A. Engel, J. Margitan, and P. A. Newman (1999), An investigation of ClO photochemistry in the chemically perturbed Arctic vortex, *J. Atmos. Chem.*, *32*, 61–81.
Plenge, J., S. Kühl, B. Vogel, R. Müller, F. Stroh, M. von Hobe, R. Flesch, and E. Rühl (2005), Bond strength of chlorine peroxide, *J. Phys. Chem.*, *109*, 6730–6734.
Pope, F. D., J. C. Hansen, K. D. Bayes, R. R. Friedl, and S. P. Sander (2007), The ultraviolet absorption spectrum of chlorine peroxide, ClOOCl, *J. Phys. Chem.*, *111*, 4322–4332.
Randel, W. J. (1987), Global atmospheric circulation statistics, 1000-1 mb, *Tech. Rep. NCAR/TN-295+STR*, Natl. Cent. for Atmos. Res., Boulder, Colo.
Rex, M., et al. (2002), Chemical depletion of Arctic ozone in winter 1999/2000, *J. Geophys. Res.*, *107*(D20), 8276, doi:10.1029/2001JD000533.
Rodgers, C. D. (2000), *Inverse Methods for Atmospheric Sounding*, World Scientific, Singapore.
Salawitch, R. J., S. C. Wofsy, and M. B. McElroy (1988), Chemistry of OClO in the Antarctic stratosphere: Implications for bromine, *Planet. Space Sci.*, *36*, 213–224.
Salawitch, R. J., et al. (2002), Chemical loss of ozone during the Arctic winter of 1999/2000: An analysis based on balloon-borne observations, *J. Geophys. Res.*, *107*(D20), 8269, doi:10.1029/2001JD000620.
Sander, S. P., et al. (2003), Chemical kinetics and photochemical data for use in atmospheric studies, *Tech. Rep. 02-25*, Jet Propul. Lab., Pasadena, Calif.
Sander, S. P., et al. (2006), Chemical kinetics and photochemical data for use in atmospheric studies, *Tech. Rep. 06-2*, Jet Propul. Lab., Pasadena, Calif.
Sander, S. P., et al. (2009), Chemical kinetics and photochemical data for use in atmospheric studies, *Tech. Rep. 09-31*, Jet Propul. Lab., Pasadena, Calif.
Sander, S. P., et al. (2011), Chemical kinetics and photochemical data for use in atmospheric studies, *Tech. Rep. 10-06*, Jet Propul. Lab., Pasadena, Calif.
Santee, M. L., G. L. Manney, W. G. Read, L. Froidevaux, and J. W. Waters (1996), Polar vortex conditions during the 1995–96 Arctic winter: MLS ClO and HNO_3, *Geophys. Res. Lett.*, *23*, 3207–3210.
Santee, M. L., G. L. Manney, L. Froidevaux, R. W. Zurek, and J. W. Waters (1997), MLS observations of ClO and HNO_3 in the 1996–97 Arctic polar vortex, *Geophys. Res. Lett.*, *24*, 2713–2716.
Santee, M. L., S. P. Sander, N. J. Livesey, and L. Froidevaux (2010), Constraining the chlorine monoxide (ClO)/chlorine peroxide (ClOOCl) equilibrium constant from Aura Microwave Limb Sounder measurements of nighttime ClO, *Proc. Natl. Acad. Sci. U.S.A.*, *107*, 6588–6593, doi:10.1073/pnas.0912659107.
Schoeberl, M. R., and L. C. Sparling (1995), Trajectory modeling, in *Diagnostic Tools in Atmospheric Physics, Proc. Int. Sch. Phys. Enrico Fermi*, vol. 124, edited by G. Fiocco and G. Visconti, pp. 289–305, IOS Press, Amsterdam.
Schofield, R., et al. (2008), Polar stratospheric chlorine kinetics from a self-match flight during SOLVE-II/EUPLEX, *Geophys. Res. Lett.*, *35*, L01807, doi:10.1029/2007GL031740.
Shindell, D. T., and R. L. deZafra (1996), Chlorine monoxide in the Antarctic spring vortex: 2. A comparison of measured and modeled diurnal cycling over McMurdo Station, 1993, *J. Geophys. Res.*, *101*, 1475–1487.
Solomon, S., R. R. Garcia, F. S. Rowland, and D. J. Wuebbles (1986), On the depletion of Antarctic ozone, *Nature*, *321*, 755–758.
Stratospheric Processes and their Role in Climate (SPARC) (2009), The role of halogen chemistry in polar stratospheric ozone depletion, *Tech. Rep.*, Stratospheric Processes and their Role in Climate Project, Cambridge.
Stimpfle, R. M., D. M. Wilmouth, R. J. Salawitch, and J. G. Anderson (2004), First measurements of ClOOCl in the stratosphere: The coupling of ClOOCl and ClO in the Arctic polar vortex, *J. Geophys. Res.*, *109*, D03301, doi:10.1029/2003JD003811.
Suminska-Ebersoldt, O., et al. (2012), ClOOCl photolysis at high solar zenith angles: Analysis of the RECONCILE self-match flight, *Atmos. Chem. Phys.*, *12*, 1353–1365.
Toohey, D. W., J. G. Anderson, W. H. Brune, and K. R. Chan (1990), In situ measurements of BrO in the Arctic stratosphere, *Geophys. Res. Lett.*, *17*, 513–516.
Toon, G. C. (1991), The JPL Mk IV interferometer, *Opt. Photonics News*, *2*, 19–21.
Tripathi, O. P., et al. (2006), High resolution simulation of recent Arctic and Antarctic stratospheric chemical ozone loss compared to observations, *J. Atmos. Chem.*, *55*, 205–226.
Urban, J. (1998), Measurements of the stratospheric trace gases ClO, HCl, O_3, N_2O, H_2O, and OH using airborne submm-wave radiometry at 650 and 2500 GHz, *Reports on Polar Research*, Alfred-Wegener-Institute for Polar and Marine Research, Bremerhaven, Germany.
Vogel, B., J.-U. Grooß, R. Müller, T. Deshler, D. S. Karhu, J. McKenna, M. Müller, D. Toohey, G. C. Toon, and F. Stroh (2002), Vertical profiles of activated ClO and ozone loss in the Arctic vortex in January and March, 2000: In situ observations and model simulations, *J. Geophys. Res.*, *107*(D22), 8334, doi:10.1029/2002JD002564, [printed 108(D5), 2003].
Vömel, H., D. W. Toohey, T. Deshler, and C. Kröger (2001), Sunset observations of ClO in the Arctic polar vortex and implications for ozone loss, *Geophys. Res. Lett.*, *28*, 4183–4186.
von Hobe, M., J.-U. Grooß, S. Müller, R. Hrechanyy, U. Winkler, and F. Stroh (2005), A re-evaluation of the ClO/Cl_2O_2 equilibrium constant based on stratospheric in-situ observations, *Atmos. Chem. Phys.*, *5*, 693–702.
von Hobe, M., R. J. Salawitch, T. Canty, H. Keller-Rudek, G. K. Moortgat, J.-U. Grooß, R. Müller, and F. Stroh (2007), Understanding the kinetics of the ClO dimer cycle, *Atmos. Chem. Phys.*, *7*, 3055–3069.
von Hobe, M., F. Stroh, H. Beckers, T. Benter, and H. Willner (2009), The UV/Vis absorption spectrum of matix-isolated dichlorine peroxide, ClOOCl, *Phys. Chem. Chem. Phys.*, *11*, 1571–1580.
von König, M. (2001), *Chlorine Activation and PSC Formation in the Arctic Stratosphere*, Berichte aus dem Institut für Umweltphysik, Universität Bremen, Logos Verlag, Berlin, Germany.

von König, M., H. Bremer, V. Eyring, A. Goede, H. Hetzheim, Q. Kleipool, H. Küllmann, and K. Künzi (2000), An airborne submm radiometer for the observation of stratospheric trace gases, in *Microwave Radiometry and Remote Sensing of the Earth's Surface and Atmosphere*, edited by P. Pampaloni and S. Paloscia, pp. 409–415, VSP, Utrecht.

Wetzel, G., H. Oelhaf, F. Friedl-Vallon, O. Kirner, A. Kleinert, G. Maucher, H. Nordmeyer, J. Orphal, and R. Ruhnke (2012), Diurnal variations of reactive chlorine and nitrogen oxides observed by MIPAS-B inside the January 2010 Arctic vortex, *Atmos. Chem. Phys.*, *12*, 6581–6592.

Wilmouth, D. M., R. M. Stimpfle, J. G. Anderson, J. W. Elkins, D. F. Hurst, R. J. Salawitch, and L. R. Lait (2006), Evolution of inorganic chlorine partitioning in the Arctic polar vortex, *J. Geophys. Res.*, *111*, D16308, doi:10.1029/2005JD006951.

Wilmouth, D. M., T. F. Hanisco, R. M. Stimpfle, and J. G. Anderson (2009), Chlorine catalyzed ozone destruction: Cl atom production from ClOOCl photolysis, *J. Phys. Chem.*, *113*, 14,099–14,108.

World Meteorological Organization (WMO) (1986), *Atmospheric Ozone: 1985*, Global Ozone Research and Monitoring Project Report No. 16, World Meteorological Organization, Geneva, Switzerland.

World Meteorological Organization (WMO) (2010), *Scientific Assessment of Ozone Depletion: 2010*, Global Ozone Research and Monitoring Project Report No. 52, World Meteorological Organization, Geneva, Switzerland.

Young, I. A. K., R. L. Jones, and F. D. Pope (2014), The UV and visible spectra of chlorine peroxide: Constraining the atmospheric photolysis rate, *Geophys. Res. Lett.*, *41*, 1781–1788, doi:10.1002/2013GL058626.